Behavioral and neural markers of visual configural processing in social scene perception

Etienne Abassi, Liuba Papeo

NeuroImage 260 (2022) 119506

Contents lists available at ScienceDirect

NeuroImage

journal homepage: www.elsevier.com/locate/neuroimage

Behavioral and neural markers of visual configural processing in social scene perception

Etienne Abassi*, Liuba Papeo

Institut des Sciences Cognitives—Marc Jeannerod, UMR5229, Centre National de la Recherche Scientifique (CNRS) and Université Claude Bernard Lyon 1, 67 Bd. Pinel, 69675 Bron France

ARTICLE INFO

Keywords:
Configural visual processing
Scene perception
fMRI
Individual differences
Autism
Brain-behavior mapping

ABSTRACT

Research on face perception has revealed highly specialized visual mechanisms such as configural processing, and provided markers of interindividual differences –including disease risks and alterations– in visuo-perceptual abilities that traffic in social cognition. Is face perception unique in degree or kind of mechanisms, and in its relevance for social cognition? Combining functional MRI and behavioral methods, we address the processing of an uncharted class of socially relevant stimuli: minimal social scenes involving configurations of two bodies spatially close and face-to-face as if interacting (hereafter, facing dyads). We report category-specific activity for facing (*vs.* non-facing) dyads in visual cortex. That activity shows face-like signatures of configural processing –i.e., stronger response to facing (*vs.* non-facing) dyads, and greater susceptibility to stimulus inversion for facing (*vs.* non-facing) dyads–, and is predicted by performance-based measures of configural processing in visual perception of body dyads. Moreover, we observe that the individual performance in body-dyad perception is reliable, stable-over-time and correlated with the individual social sensitivity, coarsely captured by the Autism-Spectrum Quotient. Further analyses clarify the relationship between single-body and body-dyad perception. We propose that facing dyads are processed through highly specialized mechanisms –and brain areas–, analogously to other biologically and socially relevant stimuli such as faces. Like face perception, facing-dyad perception can reveal basic (visual) processes that lay the foundations for understanding others, their relationships and interactions.

1. Introduction

Few functions of the human brain have been explored as much and deeply as the visual processing of faces. And few visual functions appear as vital for social life as face processing. Face processing underlies detection, recognition and identification of conspecifics, and encoding of visual information that provides the basis for attributing states, traits, goals and intentions to others, and regulating one's own behavior in social contexts (Baron-Cohen, 1997; Atkinson et al., 2011). It is therefore not surprising that highly efficient and specialized mechanisms exist for face perception, in the human visual system.

One of the most robust markers of face specialization is the *face inversion effect* (FIE), a disproportionate cost in processing a face inverted upside-down relative to a face in the canonical upright orientation (Yin, 1969). The FIE has revealed a visual mechanism, the so-called configural processing, that treats the face not as a set of parts (all present in both upright and inverted stimuli), but as a perceptual unit with a specific configuration (*i.e.*, eyes above mouth) that, when disrupted by inversion, yields detrimental effects on recognition (Tanaka and Farah, 1993; Maurer et al., 2002). The FIE is thus defined as a disproportionate (*i.e.*, statistically larger) cost of stimulus inversion for faces than for other familiar objects (Robbins and Mckone, 2007). While the inversion effect is not the only marker of configural processing, it is the most investigated, the largest and the most reliable among other behavioral markers such as the composite, part-whole and contrast negation effect (Bruyer, 2011; see also Rezlescu et al., 2017), and is also reliably detectable in neural activity, using functional MRI (fMRI) (Yovel and Kanwisher, 2005) or electroencephalography (Rossion et al., 1999, 2000; Sadeh and Yovel, 2010).

Besides revealing important aspects of visual functioning, the sensitivity to face inversion is reliable and stable over time at the intraindividual level, and can highlight interindividual differences that capture the normal variability in the general population, as well as disease risks and alterations in visual perception (Duchaine and Nakayama, 2006; Yovel et al., 2014), and in socially relevant cognitive abilities (Wyer et al., 2012; Neuhaus et al., 2016; Webb et al., 2017). Reduced sensitivity to face inversion –and atypical face processing in general– is seen in developmental disorders that affect social cognition such as the autism spectrum disorder (ASD) (Farroni and Senju, 2011; Di Giorgio et al., 2016; Neuhaus et al., 2016; Hadad et al., 2019; Van der Donck et al., 2019; Vettori et al., 2019; Laycock et al., 2020), although with high variability within the ASD population and no consen-

* Corresponding author.
E-mail address: etienne.abassi@gmail.com (E. Abassi).

https://doi.org/10.1016/j.neuroimage.2022.119506.
Received 8 October 2021; Received in revised form 18 July 2022; Accepted 21 July 2022
Available online 22 July 2022.

sus on the neurofunctional basis of the alteration (Brambilla et al., 2003; Johnson, 2004; Dawson et al., 2005; Simmons et al., 2009; Cook et al., 2012).

Is face perception unique in degree or kind of cognitive and neural mechanisms, and in its relevance for social cognition? Other visual stimuli that also support social cognitive tasks, such as bodies and biological motion (Atkinson et al., 2011), may recruit analogous mechanisms (Reed et al., 2006; Troje and Westhoff, 2006). For example, the inversion effect has been reported in single body perception (body inversion effect or BIE; Reed et al., 2003, 2006), both in the behavioral performance, and in the electroencephalography signal (Stekelenburg and De Gelder, 2004; Orlandi and Proverbio, 2020; Adibpour et al., 2021). However, other behavioral and fMRI studies have shown inconsistent results, questioning whether the inversion effect provides a reliable measure of body perception, and whether body perception recruits configural processing at all (Brandman and Yovel, 2012, 2016; but see Axelsson et al., 2022). Therefore, faces so far remain the best understood case of visual specialization mediated by configural processing.

More recent research indicates an uncharted class of stimuli, whose visual processing might be analogous to faces. Members of this class are two-body shapes, that is, configurations of two bodies spatially close and face-to-face, as is (proto)typical of a social interaction (Papeo et al., 2017; Papeo, 2020). Much of what we learn about social life, and how we regulate our social behavior *here and now*, depends on the observation of people interacting with people (Quadflieg and Koldewyn, 2017; Powell and Spelke, 2018). Thus, the visual specialization for face-to-face body dyads (hereafter, facing dyads) might respond to the need for efficient detection and recognition of social interaction in the cluttered and crowded visual world.

It has been suggested that visual processing of facing dyads shares with face processing a particular sensitivity to inversion: In fast visual categorization (*i.e.*, discrimination of bodies from other objects), subjects' performance drops dramatically for inverted facing dyads, relative to the same dyads presented upright (Papeo et al., 2017; Papeo and Abassi, 2019). The cost of inversion for facing dyads is significantly larger than the cost of inversion for identical bodies in a non-facing configuration (*e.g.*, back-to-back bodies), an effect known as the two-body inversion effect (2BIE).

What is the two-body inversion effect? The present study asked whether the 2BIE could be *a)* an index of visual specialization mediated by configural processing, and *b)* a reliable measure of the individual visuoperceptual functions that traffic in social perception and cognition.

To address the first question, we tested whether activity in person-perception (face- and body-specific) visual areas of the occipitotemporal cortex showed two well established signatures of configural processing during perception of facing dyads. The first neural signature of configural face processing is greater activity for faces relative to scrambled or scattered faces (Brandman and Yovel, 2016). Thus, if facing dyads recruit configural processing, they should evoke greater activity in visual areas, relative to their scattered counterparts, *i.e.*, stimuli featuring the same parts (bodies) in a non-facing configuration. The second signature of configural processing targeted here is the inversion effect: We studied whether the 2BIE captured in the subjects' behavior predicts the activity of visual areas in response to upright *vs.* inverted dyads, just like the FIE predicts the response to upright *vs.* inverted faces in the face-specific visual cortex (Yovel and Kanwisher, 2005). To test these effects, we recorded neural activity using fMRI, while healthy subjects viewed upright or inverted facing and non-facing dyads. On a different day, the same subjects performed a visual categorization task to measure the behavioral 2BIE (Papeo et al., 2017). We tested the visual specificity of the whole-dyad configuration considering both the difference in neural activity for upright facing *vs.* non-facing dyads, and the difference in the effect of inversion for facing *vs.* non-facing dyads (*i.e.*, whether neural activity mirrored the behavioral 2BIE), in person-perception visual areas, and in the whole brain. We repeated the same analyses on an independent set of data, collected during the presentation of upright or inverted single bodies (and non-body objects as a control). With this second study, we aimed to shed light on the relationship between body and body-dyad processing, testing whether the two types of stimuli give rise to comparable effects.

To address the second question concerning the relationship between 2BIE and interindividual differences, subjects performed the visual categorization task a second time after weeks, so that we could estimate the stability of the 2BIE over time. They also completed the Autism-Spectrum Quotient Test (AQ), a measure of the autism-spectrum traits, sensitive to interindividual differences in the general population, with respect to socially relevant cognitive abilities (Baron-Cohen et al., 2001; Ruzich et al., 2015). With caution due to a small sample size for correlational analyses, we used this dataset to begin exploring the test-retest reliability of the 2BIE, and the relationship between the 2BIE and the AQ. We aimed to provide first-pass indication that the way in which individuals process social scenes can capture individual differences in the visuoperceptual foundations of social cognition.

2. Material and Methods

2.1. Participants

Thirty subjects took part in the fMRI study (16 female; mean age 24.8 years ± 4.6 *SD*). This number respected the sample size required to obtain a difference of activity for facing *vs.* non-facing dyads in body-perception visual cortex, comparable to a previous study with similar task and design (required sample size = 30, for Cohen's $d = 0.692$ with power = 0.95, alpha = 0.05; Abassi and Papeo, 2020). All subjects had normal or corrected-to-normal vision and reported no history of psychiatric or neurological disorders, or use of psychoactive medications. They were screened for contraindications to fMRI and gave written informed consent before participation. Of the 30 subjects who enrolled in the fMRI experiment, 23 agreed to come back twice, to take part in two sessions of the behavioral study (13 females; mean age 24.6 years ± 4.5 *SD*). This number respected the sample size required to obtain a 2BIE comparable to previous research with similar task and design (required sample size = 22, for Cohen's $d = 0.824$ with power = 0.95, alpha = 0.05; Abassi and Papeo, 2020). From behavioral and fMRI data analyses, we excluded one subject for whom average performance in the behavioral task was >3 *SD* above the group mean. Thus, the final fMRI analyses included 29 participants, and the final behavioral analyses included 22 participants. This study was approved by the local ethics committee (CPP Sud Est V, CHU de Grenoble).

2.2. Stimuli

2.2.1. Behavioral study

Sixteen grayscale renderings of single human bodies in profile view and various biomechanically possible poses, were created and edited with Daz3D (Daz Productions, Salt Lake City) and the Image Processing Toolbox of MATLAB (The MathWorks Inc, Natick, Massachusetts). As many bodies were obtained by flipping horizontally each unique body, which yielded to a total of 32 single bodies. Sixteen facing dyads were created from the 32 single bodies, and then they were horizontally flipped to create 16 new dyads, for a total of 32 facing dyads. Non-facing dyads were created by swapping the position of the two bodies in each facing dyad (*i.e.*, the body on the left side was moved to the right side and *vice versa*). The distance between bodies (*i.e.*, the distance between the two closest points of the two bodies in a dyad) was matched across facing and non-facing stimuli ($\text{mean}_{\text{facing}} = 82.88$ pixels ± 13.76 *SD*; $\text{mean}_{\text{non-facing}} = 83.06 \pm 13.86$ *SD;* $t(15) = 1.00$; $p > 0.250$). For single-body stimuli, the center of image corresponded to the center of the body, defined as the mid-point between the most extreme point on the left and on the right along the *x*-axis. For dyads, the center of the image was between, and at equal distance from, the centers of the two bounding

boxes that contained each body. In summary, the final stimulus set included 96 stimuli: 32 single bodies, 32 facing dyads and 32 non-facing dyads, differing only for the relative spatial positioning of the two bodies. Another set of stimuli included 96 images of single chairs (32) and pairs of chairs (32 facing and 32 non-facing). Chair-stimuli were created from 16 grayscale exemplars of chairs and their horizontally flipped version, combined in 16 pairs of facing pairs and their flipped version, and 16 pairs of non-facing chairs and their flipped version. All body- and chair-stimuli were inverted upside-down, yielding a total of 384 stimuli presented against a light gray background. The same number of masking stimuli was created, consisting of high-contrast Mondrian arrays (11° x 10°) of grayscale circles of variable diameter (0.4°-1.8°).

2.2.2. fMRI study

The fMRI study involved the 192 (upright and inverted) body-stimuli used in the behavioral study (64 single bodies, 64 facing dyads and 64 non-facing dyads), in addition to the same 32 single chairs and a new set of 32 machines. Images in the last set depicted one of eight electronic devices (four automated teller machine, and four game machines; *i.e.*, slot machines or arcade game machines) presented in lateral view upright (N=8) and inverted (N=8), and their horizontally flipped version, upright (N=8) and inverted (N=8).

2.3. Procedures

2.3.1. Behavioral study

Visual categorization task. The behavioral task was a basic-level visual categorization requiring subjects to report, for each trial, whether they had seen bodies or chairs (Fig. 1a). This task was chosen because previous studies had shown that, with this task, the inversion effect for facing bodies: *a)* is significantly larger than the inversion effect for non-facing bodies (and for pairs of chairs), mimicking the pattern reported for upright and inverted faces, compared to upright and inverted objects; *b)* falls within the range of the magnitude of the FIE and BIE (Papeo et al., 2017; Papeo and Abassi, 2019; Abassi and Papeo, 2020). Moreover, using single bodies, the same task was shown to evoke the classic pattern of the body-inversion with a larger drop in the response accuracy for inverted bodies, than for inverted non-body objects (*i.e.*, chairs). In sum, these circumstances suggest that the current task is effective in capturing the difference in the visual processing of facing *vs.* non-facing dyads. Moreover, relative to other tasks more commonly used to measure inversion effects (*e.g.*, face or body-posture discrimination), the current task shows the effect of body positioning (facing/non-facing), without explicit instruction to attend to the number of items (one/two), the positioning (facing/non-facing) or orientation (upright/inverted) of the stimuli.

The task included two identical runs, each containing 32 trials for each of the twelve conditions (upright and inverted single, facing and non-facing, bodies and chairs), presented in random order. Each stimulus appeared once in a run. Subjects sat on a chair, 60 cm away from a computer screen, with their eyes aligned to the center of the screen (17-in. CRT monitor; 1024 × 768 pixel resolution; 60-Hz refresh rate). Stimuli on the screen did not exceed 7° of visual angle. Each trial included the following sequence of events: blank screen (200 ms), fixation cross (500 ms), blank screen (200 ms), target stimulus (30 ms), mask (250 ms) and a final blank screen that remained until the subject gave a response. The next trial began after a variable interval between 500 and 1000 ms. For each trial, subjects had to respond by pressing one of two keys on a keyboard: "1″ with the index finger for "bodies", or "2″ with the middle finger for "chair" or *vice versa* (stimulus-response mapping was counterbalanced across participants). Every 32 trials, subjects could take a break. Two blocks of familiarization preceded the experiment. In the first block, stimuli (four per condition) were shown for 250 ms, so that the subjects could easily see them. The second block (eight trials per condition) was identical to the actual experiment. Instructions for the familiarization blocks were identical to those of the actual experiment. The experiment lasted ~40 min. Stimulus presentation and response collection (accuracy and RTs) were controlled with Psychtoolbox (Brainard, 1997) through MATLAB. Each participant took part in two sessions of the same task. The second session took place with a delay ranging from two weeks to one month after the first one (mean interval 19.8 days ± 6.1 *SD*).

Autistic-Spectrum Quotient measure. After the second behavioral session, subjects completed the 50-items Autism-Spectrum Quotient scale (AQ; Baron-Cohen et al., 2001), which measures the degree to which an adult with normal intelligence shows traits associated with the autism spectrum, in the domain of social skills, attention-switching, attention to details, communication, and imagination. Subjects responded to each item using a 4-point rating scale, ranging from "definitely agree" to "definitely disagree".

2.3.2. fMRI study

fMRI data acquisition. Imaging was conducted on a MAGNETOM Prisma 3T scanner (Siemens Healthcare). T2*-weighted functional volumes were acquired using a gradient-echo-planar imaging sequence (GRE-EPI; TR/TE = 2000/30 ms, flip angle = 80°, acquisition matrix = 96 × 92, FOV = 210 × 201, 56 transverse slices, slice thickness = 2.2 mm, no gap, multiband acceleration factor = 2 and phase encoding set to anterior/posterior direction). For the main experiment and the functional localizer task, we acquired eight runs for a total of 1546 frames per participant. Acquisition of high-resolution T1-weighted anatomical images was performed after the third functional run of the main experiment and lasted 8 min (MPRAGE; TR/TE/TI = 3000/3.7/1100 ms, flip angle = 8°, acquisition matrix = 320 × 280, FOV = 256 × 224 mm, slice thickness = 0.8 mm, 224 sagittal slices, GRAPPA accelerator factor = 2). Acquisition of two field maps was performed at the beginning of the fMRI session.

Main fMRI experiment. The fMRI data acquisition consisted of two parts: the main fMRI experiment, and a functional localizer task, which we describe below. In the main experiment, facing and non-facing dyads in upright or inverted orientation were presented over three runs, each lasting 6.83 min. Each run consisted of two sequences of 16 blocks (four blocks by condition), for a total of 32 blocks of eight second each. Blocks in the first sequence were presented in a random order, and blocks in the second sequence were presented in the counterbalanced (*i.e.*, reversed) order relative to the first sequence. Each block featured eight images of the same condition, presented in a random order. A stimulus appeared once in a block, and twice in a run (once in each sequence). Thus, each of the three runs included eight blocks per condition (24 across the whole experiment). Three additional runs of 6.83 min each featured images of single bodies and single objects presented upright or inverted. Each run included 16 blocks (eight seconds each), eight with bodies and eight with objects (four with chairs and four with machines). Each block included eight different stimuli of the same condition. Each stimulus appeared twice in a run (once in each sequence). Runs with dyads and runs with single items (bodies or objects) were presented in pseudorandom order to avoid the occurrence of more than two consecutive runs of the same stimulus group. Each run began with a warm-up block (10 s) and ended with a cool-down block (16 s), during which a central fixation cross was presented. Within a run, the onset time of each block was jittered (range of inter-block interval duration: 2–6 s; total inter-block time by runs: 128 s), using the optseq tool of Freesurfer (Fischl, 2012) for optimal jittering. During each block, a black cross was always present in the center of the screen, while stimuli appeared for 550 ms, separated by an interval of 450 ms. In the 37% of all the stimulation and fixation periods, the cross changed color (from black to red). Participants were instructed to fixate the cross throughout the experiment, detect and report the color change by pressing a button with their right index finger. This task was used to minimize eye movements and maintain vigilance in the scanner. The main experiment lasted 41 min. During fMRI, stimuli were back-projected onto a screen by a liquid crystal projector (frame rate: 60 Hz; screen resolution: 1024 × 768 pixels,

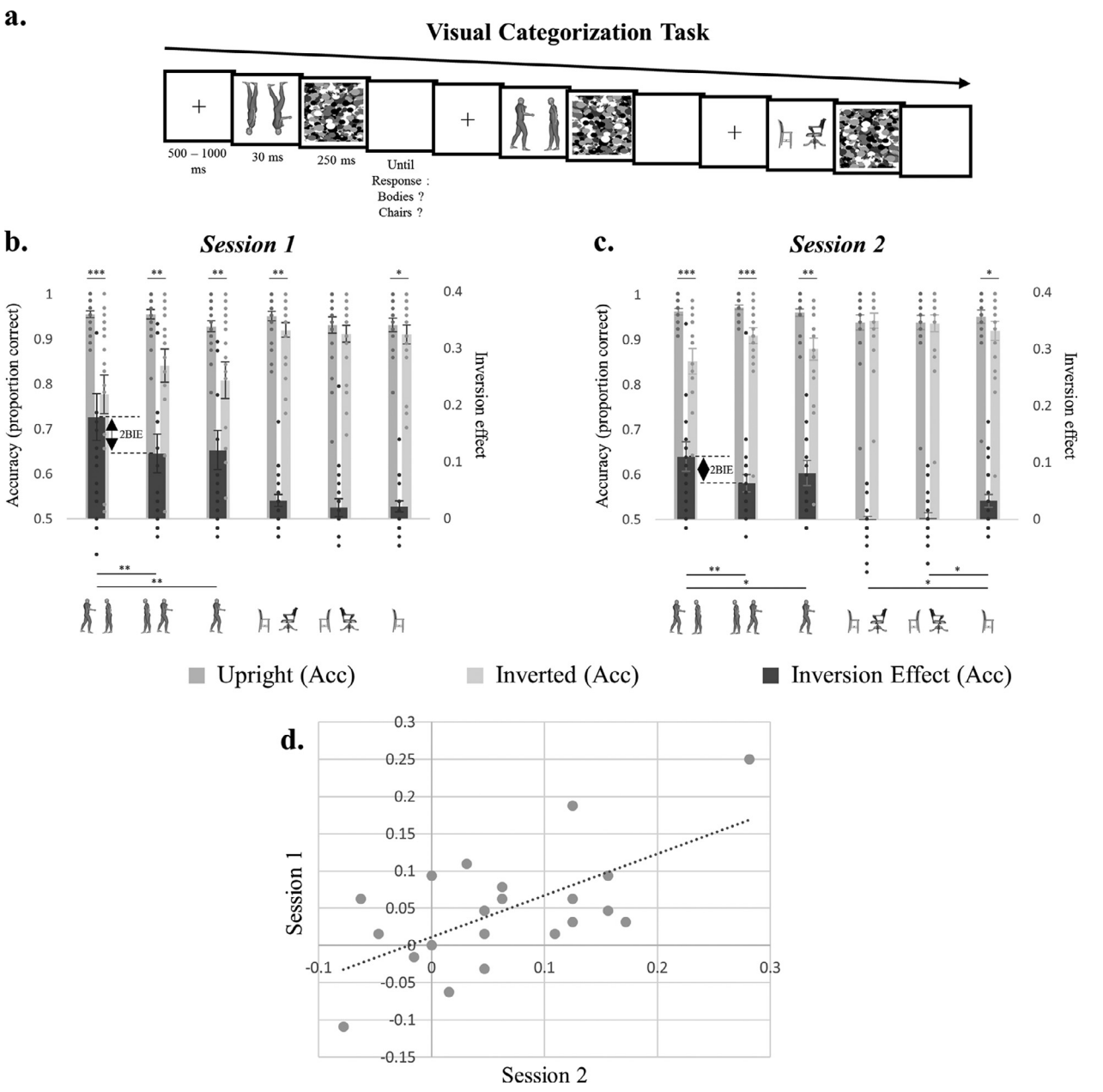

Fig. 1. Behavioral 2BIE and within-subject correlation between the two measures of the 2BIE. a. Illustration of the visual categorization task used to measure the behavioral 2BIE. b-c. Proportion of correct responses (proportion correct) and inversion effect (proportion of correct responses for upright minus inverted trials) for facing dyads, non-facing dyads and single bodies in session 1 (b), and session 2 (c). The *y*-axis on the left refers to proportion correct bars (lighter gray bars in the back); The *y*-axis on the right refers to inversion effect (darker gray bar in the front). Asterix in the upper part of the plots denote significant pairwise comparisons between proportion correct for facing *vs.* non-facing stimuli. Asterix in the bottom part of the plots denote significant pairwise comparisons of inversion effects across stimulus conditions (facing, non-facing, single). Error bars denote the within-subjects normalized standard error of the mean. Solid dots denote individual performances. d. Pearson correlation between the size of the 2BIE for the same subjects, measured in the first and second session of the visual categorization task. $^{*}p \leq 0.05$; $^{**}p \leq 0.01$; $^{***}p \leq 0.001$.

screen size: 40 × 30 cm). For all the stimuli, the center of the image overlapped with the center of the screen. Subjects, lying down inside the scanner, viewed the stimuli binocularly (~7° of visual angle) through a mirror above their head. Stimulus presentation, response collection and synchronization with the scanner were controlled with the Psychtoolbox through MATLAB.

Functional localizer task. In addition to the six experimental runs, subjects completed a functional localizer task, with stimuli and task adapted from the fLoc package (Stigliani et al., 2015). During this task, subjects saw 180 grayscale photographs of the following five object classes: 1) body-stimuli (headless bodies in various views and poses, and body parts); 2) faces (adults and children); 3) places (houses and corridors); 4) inanimate objects (various exemplars of cars and musical instruments); 5) scrambled objects. Stimuli were presented over two runs (5.27 min each). Each run began with a warm-up block (12 s) and ended with a cool-down block (16 s), and included 72 blocks of four seconds each: 12 blocks for each object class with eight images per block (500 ms per image without interruption), randomly interleaved with 12 baseline blocks featuring an empty screen. To minimize low-level differences across categories, the view, size, and retinal position of the images varied across

trials, and each item was overlaid on a 10.5° phase-scrambled background generated from another image of the set, randomly selected. During blocks containing images, some images were repeated twice, interleaved by a different image (2-back task). Participants had to press a button when they detected the repetition.

Preprocessing of fMRI data. Functional images were preprocessed and analyzed using MATLAB, in combination with SPM12 (Friston et al., 2007), the CoSMoMVPA toolbox (Oosterhof et al., 2016), the MarsBaR toolbox (Brett et al., 2002) and the MatlabTFCE toolbox (Thornton, 2016). The first four volumes of each run were discarded, taking into account initial scanner gradient stabilization (Soares et al., 2016). Preprocessing of the remaining volumes involved despiking, slice time correction, geometric distortions correction using field maps, spatial realignment and motion correction using the first volume of each run as reference. The maximum displacement after despiking was 0.74 mm on the *x*-axis ($mean_{max}$ = 0.30, *SD* = 0.18), 2.31 mm on the *y*-axis ($mean_{max}$ = 0.65, *SD* = 0.52) and 3.29 mm on the *z*-axis ($mean_{max}$ = 1.06, *SD* = 0.64), which did not exceed the Gaussian kernel of 5 mm FWHM used for the spatial smoothing before estimating the realignment parameters (Friston et al., 1996). Anatomical volumes were co-registered to the mean functional image, segmented into gray matter, white matter and cerebrospinal fluid in native space, and aligned to the probability maps in the Montreal Neurological Institute (MNI). The DARTEL method (Ashburner, 2007) was used to create a flow field for each subject and an inter-subject template, which was registered in the MNI space and used for normalization of functional images. Final steps included spatial smoothing with a Gaussian kernel of 6 mm FWHM and removing low-frequency drifts with a temporal high-pass filter (cutoff 128 s).

2.4. Analyses

2.4.1. Behavioral study

Visual categorization task. Separately for the two sessions of the task, we computed the mean proportion of correct responses (accuracy) and the median RTs for each condition, for each subject. Median RTs were computed over trials with accurate response and RTs within 3 *SD* from the individual median value (discarded RTs in session 1: 11.64% ±7.40 *SD*; in session 2: 8.59% ±6.03 *SD*). All responses were included in the accuracy analysis. Accuracy and RTs data were analyzed with 2 Category (body, chair) x 3 Stimulus (facing dyads, non-facing dyads, single bodies) x 2 Orientation (upright, inverted) repeated-measures ANOVAs. Critical comparisons were tested using pairwise *t* tests. Analyses were repeated values from each session separately.

Test-retest reliability. For each subject, we computed the 2BIE on accuracy values [$(Upright\text{-}inverted)_{facing}$-$(Upright\text{-}inverted)_{non\text{-}facing}$] for each of the two sessions. Across-session comparisons were first performed using a *t* test, ($\alpha = 0.05$, two-tail), and then with within-subjects Pearson correlation ($\alpha = 0.05$) to assess the intra-individual consistency of the 2BIE. For the latter analysis, we used a permutation test (10,000 iterations) to verify that the within-subjects correlation was higher than the correlation between any two randomly selected values (between-subjects correlations). In each iteration, the 2BIE from the first session of a subject was randomly assigned to the 2BIE of another subject in the second session and a Pearson correlation coefficient was computed. We ranked the single within-subjects correlation value on the distribution of the 10,000 between-subjects correlations values, and divided the rank by number of permutations to obtain a *p* value. We assessed whether a significant within-subject correlation was statistically higher than random between-subject correlations.

Correlation between 2BIE and AQ. We computed Spearman correlation ($\alpha = 0.05$) between the behavioral 2BIE and the AQ score of the 22 subjects who participated in both behavioral sessions. This analysis was repeated using data from session 1 and session 2 of the visual categorization task.

2.4.2. fMRI study of body-dyad processing

Whole-brain analysis. For each subject, the blood-oxygen-level-dependent (BOLD) signal of each voxel was estimated with a random-effects general linear model (RFX GLM), including four regressors for the four experimental conditions (upright and inverted facing and non-facing dyads), one regressor for fixation blocks, and six regressors for movement correction parameters as nuisance covariates. In the first analysis, the effect of the visuo-spatial configuration of bodies within a dyad was assessed, separately for the upright and inverted orientations, with a RFX GLM contrasting facing *vs.* non-facing dyads. In the second analysis, the effect of stimulus orientation was assessed, separately for facing and non-facing dyadic configurations, with a RFX GLM contrasting upright > inverted orientation. For all univariate analyses, the statistical significance of second-level (group) effects was determined using a voxelwise threshold of $p \leq 0.001$, family-wise error corrected at the cluster level.

Definition of regions of interest (ROIs). With data from the functional localizer task, we identified, for each subject, two areas of the visual occipototemporal cortex showing the highest response to body stimuli, the EBA and the fusiform body area (FBA). In addition, we localized the individual face-specific fusiform face area (FFA). The FFA was localized not only because faces were part of our stimuli, but also because this area has consistently been implicated in configural processing of faces as well as bodies (Yovel and Kanwisher, 2005; Brandman and Yovel, 2016). Finally, to control for the specificity of effects in the above ROIs, we considered two additional ROIs, the place-specific parahippocampal place area (PPA), and the early visual cortex (EVC). To define these ROIs (Fig. 3a), individual data were entered into a General Linear Model with five regressors for the five object-class conditions (bodies, faces, places, objects and scrambled objects), one regressor for baseline blocks, and six regressors for movement correction parameters as nuisance covariates. Three bilateral masks of the middle temporo-occipital gyrus (MTOG), the temporo-occipital fusiform cortex (TOFC) and the inferior parahippocampal cortex (PHC) were created using FSLeyes (McCarthy, 2022) and the Harvard-Oxford Atlas (Desikan et al., 2006) through FSL (Jenkinson et al., 2012). In addition, a bilateral mask of the EVC encompassing visual areas V1/V2 and V3v/V3d, was created using the SPM Anatomy toolbox (Eickhoff et al., 2005). Within each mask of each subject, we selected the voxels with significant activity (threshold: $p = 0.05$) for the contrasts of interest, to create ROIs: EBA in the MTOG with the contrast bodies > [objects+faces+places], FFA in the TOFC with the contrast faces > [objects+bodies+places], FBA in the TOFC with the contrast body > [objects+face+places] and PPA in the PHC with the contrast places > [objects+faces+bodies]. The EVC-ROI included all the voxels responsive to visual stimuli (contrast: [bodies+faces+places+objects+scrambled objects] > baseline). For each ROI, all of the voxels within the bilateral mask that passed the threshold, were ranked by activation level based on *t* values. The final ROIs included up to 200 best voxels across the right and left ROI (number of voxels in the EBA, FBA, FFA and EVC: 200; in the PPA: 199.86 ± 0.58 *SD*). Neural activity values used for all ROIs analyses were extracted as the percent signal change (PSC) for each condition, using the MarsBaR toolbox (Brett et. al., 2002).

ROIs analyses. Using data recorded during runs with dyads in the main fMRI experiment (N = 29), we analyzed in each ROI the effects of seeing upright or inverted facing and non-facing dyads. In particular, we performed a repeated-measures ANOVA with factors: 5 ROI (EBA, FBA, FFA, PPA and EVC) x 2 Stimulus (facing and non-facing dyads) x 2 Orientation (upright and inverted). Next, pairwise *t*-tests were used to investigate, in each ROI, the two signatures of configural processing: 1) larger response to facing than to non-facing (upright) dyads ($\alpha = 0.05$ one-tail), and 2) larger difference between upright and inverted stimuli for facing, than for non-facing dyads –i.e., the neural 2BIE ($\alpha = 0.05$, one-tail).

Brain-behavior correlation (in ROIs). We investigated whether the behavioral 2BIE, taken as a signature of the configural processing of dyads,

could predict the response to dyadic stimuli in visual cortex. This analysis was carried out within each ROI, using the PSC extracted for each condition (upright and inverted facing and non-facing dyads). First, for each subject who was included in all behavioral and fMRI sessions of the study, for each ROI, we computed a normalized measure of the neural 2BIE:

$$[(\text{Upright-Inverted})_{\text{facing}}/(\text{Upright+Inverted})_{\text{facing}}]-[(\text{Upright-Inverted})_{\text{non-facing}}/(\text{Upright+Inverted})_{\text{non-facing}}].$$

Normalized measure of activity was used to take care of inter-subjects differences in the overall magnitude of fMRI response, which are not suitable for correlation with behavioral responses (Yovel and Kanwisher, 2005). For each ROI, measures of the neural 2BIE were correlated with measures of the behavioral 2BIE (Pearson correlation, $\alpha = 0.05$). Across ROIs, correlation coefficients were compared (Steiger, 1980) using the online tool *quantpsy* (Lee and Preacher, 2013). This analysis was repeated using data from the behavioral sessions 1 and 2.

Brain-behavior correlation (in the whole-brain). For the 22 participants who participated in both the behavioral and the fMRI sessions, we used the behavioral-2BIE from the first behavioral session and we measured a neural 2BIE for each voxel in the brain. To do so, we selected all the voxels across the brain with a positive β-weight for all conditions of body dyads and, for the selected voxels, we extracted the β-weights for each condition. Then, separately for facing and non-facing dyads, we computed for each voxel the normalized inversion effects ([upright stimuli – inverted stimuli] / (upright stimuli + inverted stimuli]) and defined the neural-2BIEs as the difference in the normalize inversion effect between facing and non-facing dyads. For all participants, for each voxel, we computed the Pearson correlation between the neural-2BIE and the behavioral-2BIE. For this analysis, the statistical significance of the correlation was determined using a voxelwise threshold of $p \leq 0.05$ (one-tailed). The statistical map of Pearson correlation coefficients (Fisher-transformed) was corrected for multiple comparisons using a permutation testing approach (Nichols and Holmes, 2002) combined with threshold free cluster enhancement transformations (TFCE, Smith and Nichols, 2009) through the MatlabTFCE toolbox (permutation number = 5000, H = 2, E = 0.5, dh=0.1, Connectivity = 26, one-tailed). The same analysis was repeated using values of the behavioral-2BIE based on sessions 1 and 2 of the behavioral task, separately.

Univariate test of the single-body inversion effect (BIE). To assess the recruitment of configural processing for single bodies, we tested whether the difference in the response to upright *vs.* inverted bodies was statistically larger than a general effect of inversion that would be observed for any (non-body) stimulus. For each of the above ROIs, data recorded during the runs of the main fMRI experiment involving single bodies and objects were analyzed with a repeated-measures ANOVA with factors, 2 Category (body and object) and 2 Orientation (upright and inverted). Next, pairwise *t*-tests were used to investigate, in each ROI, the inversion effect for single bodies. In particular, we first computed the inversion effect (stronger response to upright than inverted stimuli) separately for bodies and objects ($\alpha = 0.05$, one-tail), and then tested whether the inversion effect was larger for bodies than for objects ($\alpha = 0.05$, one-tail). Finally, the magnitude of the BIE was compared with the inversion effect for facing and non-facing dyads.

Multivariate test of the single-body inversion effect (BIE). As another test of the body inversion effect, from each ROI, we extracted multivariate activity patterns for the four conditions, and performed MVPA to compute the accuracy of discrimination between upright and inverted stimuli, for bodies and objects. A larger inversion effect for bodies relative to any other object should yield higher discrimination accuracy between upright and inverted bodies, than between upright and inverted (non-body) objects (Brandman and Yovel, 2016). To do so, a support vector machine classifier was trained on 5 out of 6 runs to classify upright *vs.* inverted stimuli, and then tested on data from the remaining run. This scheme was iterated until all runs were used as testing and training sets. For each subject, for each ROI, accuracy values were averaged across all iterations, tested against chance (50% accuracy, *t*-tests, $\alpha = 0.05$, one-tail) and, finally, compared between bodies and objects (*t* tests, $\alpha = 0.05$, one-tail).

Data and Code availability statement

Data and codes for the behavior analyses and fMRI group analyses are available here: https://osf.io/pse3k/

3. Results

3.1. Processing of body dyads

3.1.1. The behavioral 2BIE

For this analysis, run over the accuracy values of the first session of the visual categorization task, the statistics are reported in Table 1. Results showed significant main effects and interactions, which were qualified by a significant three-way interaction between Category, Stimulus and Orientation. To unpack this interaction, we run two separate ANOVAs with body-trials and chair-trials. Results showed that the magnitude of the inversion effect was affected by the type of Stimulus (single, facing, non-facing) for body-stimuli, but not for chair-stimuli.

For body-stimuli, pairwise *t*-tests showed that, while the inversion effect (*i.e.*, the difference between upright *vs.* inverted stimuli) was significant for all three stimulus conditions [facing bodies: $t(21) = 4.33$, $p < 0.001$; non-facing bodies: $t(21) = 3.34$, $p = 0.003$; single bodies: $t(21) = 3.48$, $p = 0.002$], it was larger for facing bodies relative to non-facing bodies, $t(21) = 3.47$, $p = 0.002$, and single bodies, $t(21) = 3.35$, $p = 0.003$, and comparable for the last two, $t(21) = 0.39$, $p > 0.250$ (Fig. 1b). Separate analysis run over the accuracy values from session 2 gave identical results (Fig. 1c-d; Tables 1-2). Consistent with previous reports (Abassi and Papeo, 2020; Papeo et al., 2017; Papeo and Abassi, 2019), accuracy proved more sensitive than reactions times (RTs) to the effects of inversion in the current task. RT analyses gave no effects or conformed to the pattern of accuracy results (Tables S1-S2, Figure S1).

The test-retest reliability of the 2BIE was computed considering, for each subject, the two measures of the 2BIE $[(\text{Upright-inverted})_{\text{facing}}-(\text{Upright-inverted})_{\text{non-facing}}]$ measured in the behavioral session 1 and 2. We found a significant within-subjects Pearson correlation [$r(20) = 0.63$, $p = 0.002$] (Fig. 1d), which was significantly higher than any random between-subjects correlation [$p = 0.001$]. This result defines the 2BIE as a reliable, stable over time, measure of the individual visual processing of body dyads.

At the group level, there was no difference in the magnitude of the 2BIE between the first and the second session, $t(21) = 1.13$, $p > 0.250$, although accuracy was overall higher in the second session, $t(21) = 2.96$, $p = 0.008$. As the very same task and stimuli were used in the two sessions, this difference could reflect a learning effect, which can affect upright and inverted stimuli, and therefore the size of the inversion effect (Hussain et al., 2009; Laguesse et al., 2012; De Heering and Maurer, 2013). In fact, we found that the increase in accuracy tended to be higher, although not significantly, for inverted (+7.12%; facing: + 7.53 %; non-facing: + 6.82 %) than for upright (+1.21%; facing: + 0.71 %; non-facing: +1.70 %) dyads, $t(21) = 1.79$, $p > 0.087$. Given the suspect that learning effect might have changed the inversion effect in a way that is difficult to quantify, in the following analyses, we primarily relied on the results from session 1, which provided a measure of the 2BIE free from effects of perceptual learning. All the analyses however were repeated with data from session 2 and are reported in supplementary materials.

Finally, we compared, qualitatively, the size of the inversion effects for facing and non-facing dyads, as measured in the current and in three

Table 1
Results of the repeated-measures ANOVAs on accuracy values (proportion correct) for session 1 and session 2 of the behavioral task.

Category	Effect	*DF*	Session 1			Session 2		
			F	*p*	η_p^2	*F*	*p*	η_p^2
Bodies & Chairs	Cat.	1,21	4.70	0.042	0.18	0.96	*n.s.*	0.04
	Stim.	2,42	4.18	0.022	0.17	4.76	0.014	0.18
	Orient.	1,21	21.27	<0.001	0.50	16.90	<0.001	0.45
	Cat. * Stim.	2,42	6.75	0.003	0.24	6.24	0.004	0.23
	Cat. * Orient.	1,21	8.87	0.007	0.30	14.89	0.001	0.41
	Stim. * Orient.	2,42	6.13	0.005	0.23	3.96	0.026	0.16
	Cat. * Stim. * Orient.	2,42	4.45	0.018	0.17	7.89	0.001	0.27
Bodies	Stim.	2,42	7.52	0.002	0.26	6.89	0.003	0.25
	Orient.	1,21	15.05	0.001	0.42	18.00	<0.001	0.46
	Stim. * Orient.	2,42	8.74	0.001	0.29	5.77	0.006	0.22
Chairs	Stim.	2,42	0.95	*n.s.*	0.04	0.46	*n.s.*	0.02
	Orient.	1,21	1.24	*n.s.*	0.06	1.83	0.190	0.08
	Stim. * Orient.	2,42	0.98	*n.s.*	0.04	5.96	0.005	0.22

Notes. Cat. = Category; Stim. = Stimulus; Orient. = Orientation; n.s. = >0.250

Table 2
Results of the pairwise comparisons based on response accuracy values from Session 1 and 2. *T*-test statistics assessing the inversion effect (IE) for each stimulus condition (proportion correct for upright > inverted stimuli) and across stimulus conditions (facing, non-facing and single bodies).

Category	Test	Session 1		Session 2	
		t(21)	*p*	*t(21)*	*p*
Bodies	IE facing	4.33	< 0.001	4.27	< 0.001
	IE non-facing	3.34	0.003	4.15	< 0.001
	IE single	3.48	0.002	3.64	0.002
	IE facing *vs.* IE non-facing	3.47	0.002	2.87	0.009
	IE facing *vs.* IE single	3.35	0.003	2.13	0.045
	IE non-facing *vs.* IE single	0.39	*n.s.*	1.57	0.132
Chairs	IE facing	3.06	0.006	0.50	*n.s.*
	IE non-facing	1.22	0.234	0.23	*n.s.*
	IE single	2.13	0.045	2.80	0.011
	IE facing *vs.* IE non-facing	0.98	*n.s.*	0.77	*n.s.*
	IE facing *vs.* IE single	0.93	*n.s.*	2.64	0.015
	IE non-facing *vs.* IE single	0.09	*n.s.*	2.73	0.013

Notes. facing = facing dyads; non-facing = non-facing dyads; single = single bodies; n.s. = >0.250

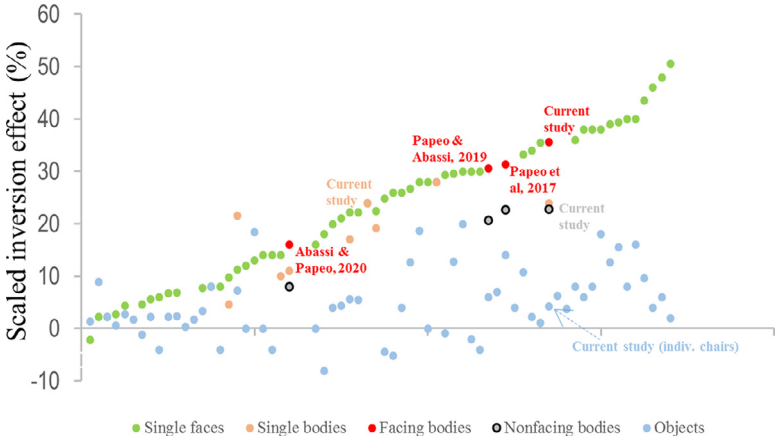

Fig. 2. Scaled inversion effect (%) for facing dyads compared to the effect for non-facing dyads, single faces, single bodies and other objects. Each point represents the scaled inversion effect measured in one of the studies reviewed in Rezlescu et al. (2016), to which we added values of the scaled inversion effect for facing and non-facing body-dyads, as measured in three previous studies and in the current one (session 1). Studies are sorted on the *x*-axis according to the size of the scaled inversion effect for each category of stimuli in each study. References in red correspond to the closest red dot and denote the size of inversion effect for facing dyads.

previous studies (Papeo et al., 2017; Papeo and Abassi, 2019; Abassi and Papeo, 2020), with the size of the inversion effects for single faces, bodies and objects, as measured in various previous studies reviewed in Rezlescu et al., 2016 (the full list of studies considered here with corresponding values for the scaled inversion effects, is provided in *Table S3*). To this end, the scaled inversion effects (%) were computed for all the studies as [(raw inversion effect)/(1-chance)], and visualized in a single plot. As shown in Fig. 2, the inversion effect for facing dyads is systematically larger than the inversion effect for non-facing dyads and closer to of the inversion effect for faces than to all other categories (single bodies and other objects). Average scaled inversion effects were (in descending order): 28.4 ±8.55 SD for facing bodies (4 studies), 22.78 ±13.78 for faces (55 studies), 18.5 ±7.07 for non-facing bodies (4 studies), 17.71 ±7.74 for single bodies (9 studies), 4.76 ±6.63 for other objects (56 studies).

3.1.2. *Neural signatures of visual configural processing*

A neural signature of configural face processing is the increased response to faces (or bodies) *vs.* scattered stimuli in category-specific visual areas of the occipitotemporal cortex (Taylor et al., 2007; Brandman and Yovel, 2016). Our results showed an analogous effect during processing of body dyads, where non-facing dyads were taken

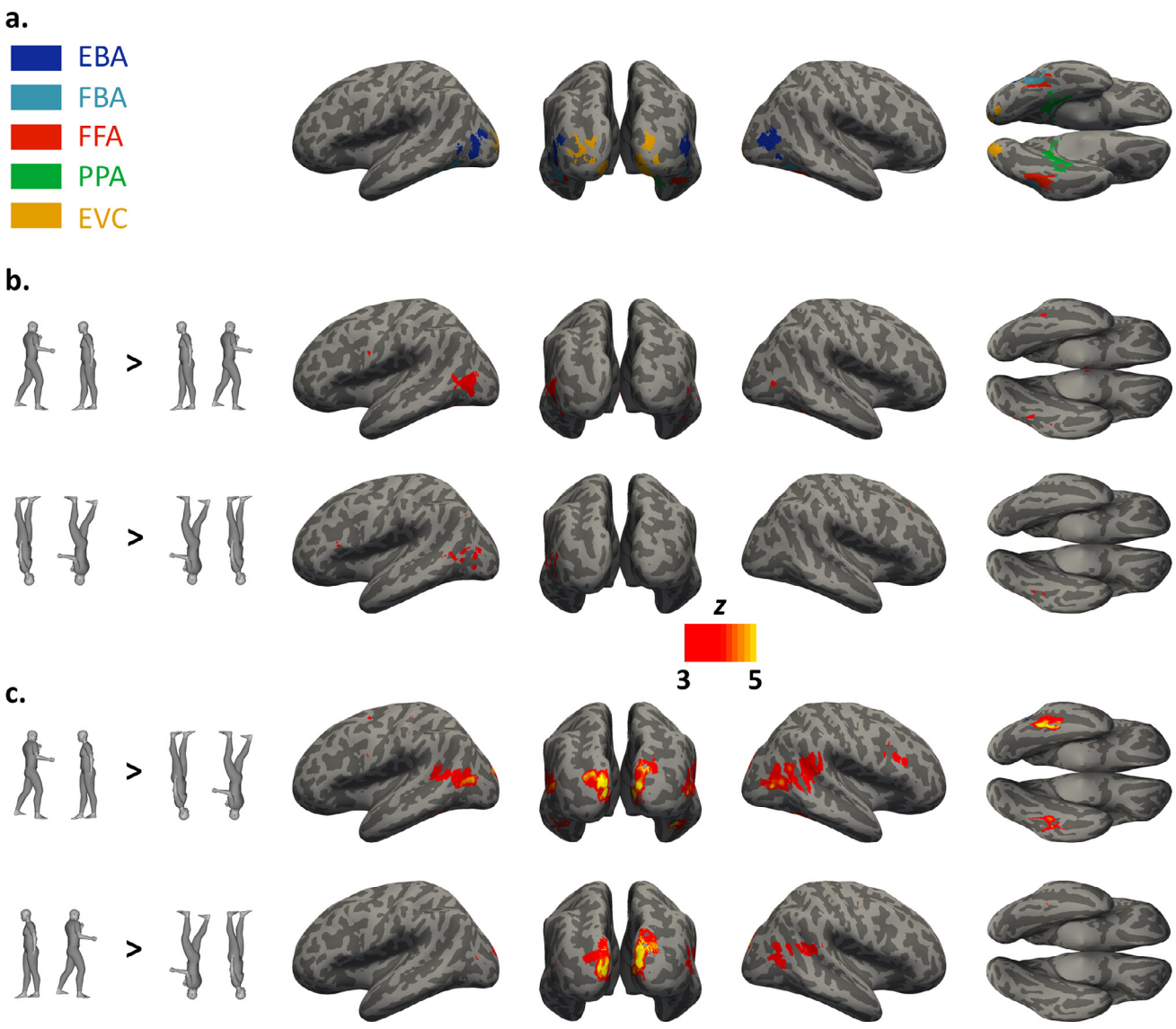

Fig. 3. Definition of Regions of Interest (ROIs) and results of whole-brain contrasts addressing the effects of configural processing in body-dyad perception a. ROI location on an inflated brain, based on fMRI data registered during the functional localizer task: EBA (extrastriate body area), FBA (fusiform body area), FFA (fusiform face area), PPA (parahippocampal place area) and EVC (early visual cortex). Group-level clusters are shown for illustration purposes. b. Group random-effect maps (n = 29) for the contrast upright facing > non-facing dyads (upper row) and inverted facing > non-facing dyads (lower row). c. Group random-effect maps (n = 29) for the contrast upright > inverted facing dyads (upper row) and upright > inverted non-facing dyads (lower row). The color bar indicates uncorrected z values.

as the scattered counterpart of facing-dyad configurations. Converging evidence for increased response to facing *vs.* non-facing dyads was obtained with the whole-brain and ROI analyses.

The whole-brain contrast [upright facing > non-facing dyads], based on data collected during the main fMRI experiment, showed an effect in a cluster centered in the left posterior middle temporal gyrus, extending into the lateral occipital cortex and overlapping with the body-specific extrastriate body area (EBA) [MNI peak coordinates: -50 -72 12; peak z-value = 3.96; peak p-value ⟨ 0.001; cluster size = 336; p = 0.013, FWE-corrected; see Fig. 3b]. For the contrast [inverted facing ⟩ non-facing dyads], no clusters survived the FWE correction.

The above effect of body positioning in the occipitotemporal cortex was confirmed by the ROI analysis. A 5 ROIs x 2 Stimulus (facing, non-facing) x 2 Orientation (upright, inverted) ANOVA showed effects that were qualified by a significant three-way interaction (Table 3). The interaction showed that the stimulus inversion affected the neural response to facing and non-facing dyads in a different way, across the ROIs. To unpack this interaction, in each ROI, we assessed the two signatures of configural processing targeted here: *1)* a larger response to facing than to non-facing (upright) dyads (Fig. 4a), and *2)* a larger difference between upright and inverted stimuli for facing than for non-facing dyads (*i.e.*, the neural 2BIE) (Fig. 4b). We found stronger response to upright facing than non-facing dyads in the FFA, $t(28) = 3.41$, $p < 0.001$, the EBA, $t(28) = 3.52$, $p < 0.001$, and the FBA, $t(28) = 2.51$, $p = 0.009$, but not in the PPA, $t(28) = 0.09$, $p > 0.250$, and EVC, $t(28) = 0.08$, $p > 0.250$. Moreover, we found a larger inversion effect for facing than for non-facing dyads in the FFA, $t(28) = 2.36$, $p = 0.013$, and a trend in the same direction in the EBA, $t(28) = 1.49$, $p = 0.073$. No other ROI showed a similar effect or trend [FBA: $t(28) = 0.88$, $p = 0.192$; PPA: $t(28) = 0.67$, $p > 0.250$; EVC: $t(28) = 0.74$; p = 0.234] (for whole-brain contrasts addressing the effect of inversion see Fig. 3c; *Table S4*).

In sum, we found higher activity for facing than non-facing dyads, selectively in the EBA, FBA and FFA, that is, in category-specific areas relevant for the processing of the experimental stimuli. Moreover, neural responses showed a pattern consistent with the behavioral 2BIE (*i.e.*, a larger difference between upright and inverted stimuli for fac-

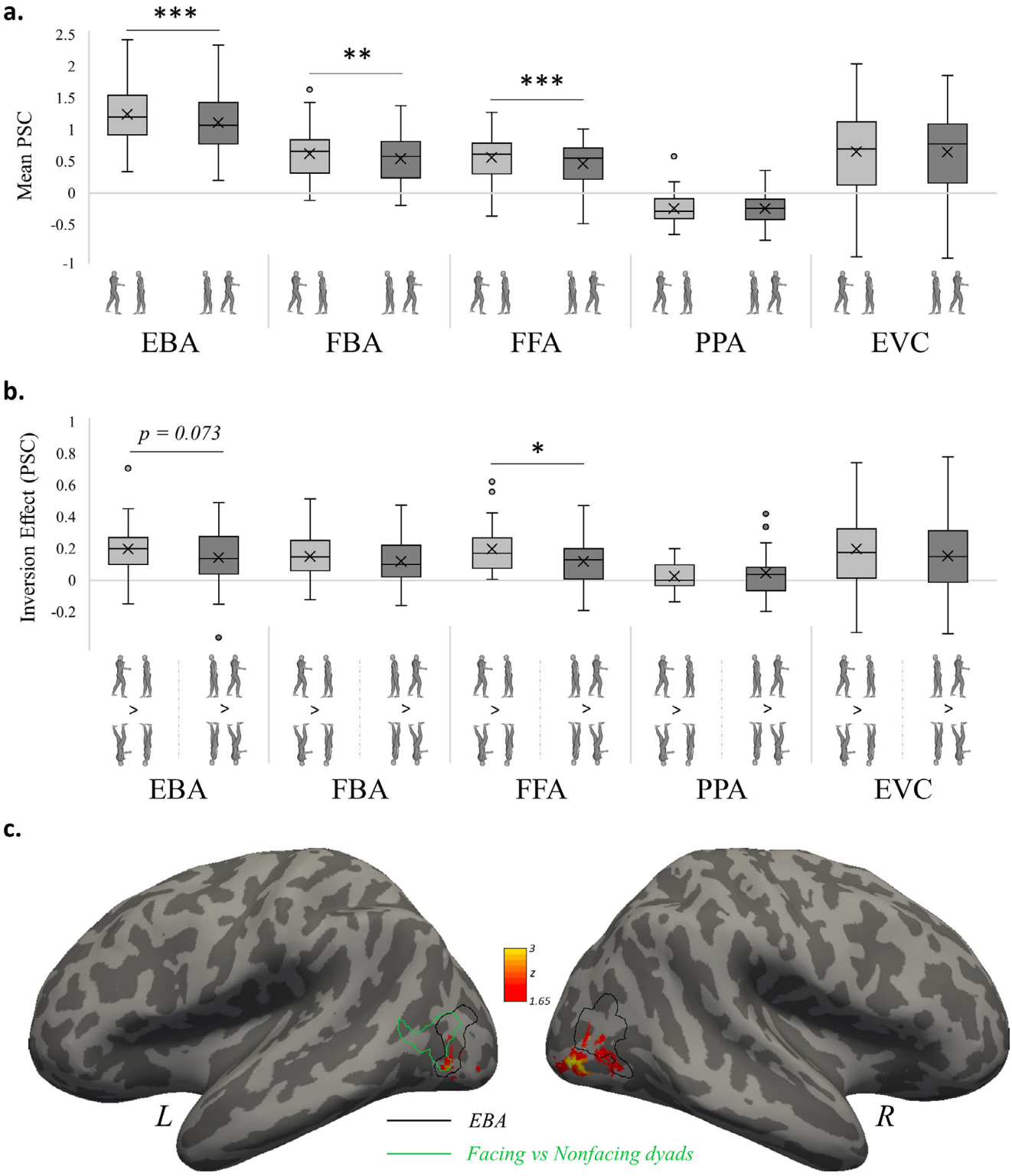

Fig. 4. Neural markers of configural processing for body dyads. a. Activity (percentage of signal change, PSC) for facing and non-facing dyads in each ROI. Higher activity for facing (*vs.* non-facing) dyads is taken as marker of configural processing. b. Difference in neural activity (PSC) between upright and inverted stimuli (*i.e.*, inversion effect) for facing and non-facing dyads, in each ROI. Greater inversion effect for facing than non-facing dyads is taken as another marker of configural processing. Error bars denote the within-subjects normalized SEM. $^{*}p \leq 0.05$; $^{**}p \leq 0.01$; $^{***}p \leq 0.001$; All tests are one-tail *t*-tests. Analyses were performed in the individually defined ROIs. c. Statistical map (uncorrected) representing the results of the correlation between the neural 2BIE and the behavioral 2BIE computed in each body-responsive voxel across the brain. The color bar indicates *z* values. The region delimited by the black line corresponds to the EBA found with the group-level contrast [bodies > (objects+faces+places)] using data recorded during the functional localizer task. The region delimited by the green line corresponds to the group-level cluster found with the contrast [facing > non-facing dyads] in the analysis of data recorded during the main fMRI experiment.

Table 3
Results of the repeated-measures ANOVAs on neural responses (PSC) for the fMRI session with dyads.

Effect	*DF*	*F*	*p*	η_p^2
ROI	4112	69.89	< 0.001	0.71
Stim.	1,28	4.85	0.036	0.15
Orient.	1,28	23.92	< 0.001	0.46
ROI * Stim.	4112	12.74	< 0.001	0.31
ROI * Orient.	4112	10.65	< 0.001	0.28
Stim. * Orient.	1,28	1.09	*n.s.*	0.03
ROI * Stim. * Orient.	4112	2.69	0.035	0.09

Notes. Cat. = Category; Stim. = Stimulus; Orient. = Orientation; n.s. = >0.250

ing than for non-facing dyads) in the FFA and EBA. The relationship between the behavioral and neural 2BIE was further investigated as follows.

3.1.3. Brain-behavior correlation

The current analysis investigated whether the behavioral 2BIE, taken as a signature of configural processing of body dyads, could predict the response to dyadic stimuli in visual cortex, with the caveat of a small sample size for correlational analysis. This analysis was carried out within the ROIs and across the whole-brain. First, Pearson correlations computed between the neural 2BIE and the behavioral 2BIE from session 1 (accuracy data) revealed a significant effect in the bilateral EBA, $r(20) = 0.44$, p = 0.039, but not in other ROIs [FBA: $r(20) = 0.16$, p > 0.250; FFA: $r(20) = 0.28$, p = 0.214; PPA: $r(20) = -0.24$, p > 0.250; EVC: $r(20) = 0.27$, p = 0.228]. Using an alternative regression approach to compute the inversion effect (see DeGutis et al., 2013), results did not change (*Supplementary Information 1)*. Identical results were found when, for each region, we created separate ROIs in the left and right hemisphere (*Supplementary Information 2*). The correlation coefficient for the EBA, however, was not statistically different from the coefficients of correlation in the other ROIs (EBA *vs.* FBA: $p = 0.084$; *vs.* FFA: $p > 0.250$; *vs.* PPA: $p = 0.057$; *vs.* EVC: $p > 0.250$). For this analysis, we considered the performance of subjects in session 1 of the behavioral task, as that was devoid of learning effects. The same analysis using data from session 2 confirmed a significant brain-behavior correlation in the right EBA only (*Supplemental Information 3*).

A separate data-driven analysis provided converging evidence for a 2BIE-*like* pattern of response in the EBA. For each subject, for each voxel responsive to body stimuli across the whole brain, we computed the neural 2BIE and performed the correlation with the behavioral 2BIE. A significant brain-behavior correlation was found in a bilateral cluster in the lateral occipital cortex, encompassing the EBA and extending more posteriorly into the occipital cortex [(right peak MNI coordinates: 44 -82 -6; peak *z*-value = 3.43; peak *p*-value < 0.001; cluster size = 219), (left peak MNI coordinates: -48 -74 2; peak *z*-value = 2.83; peak *p*-value = 0.002; cluster size = 52)] (Fig. 4c). The effect appeared bilaterally but more strongly in the right hemisphere, where it survived the correction for multiple comparisons (peak MNI coordinates: 44 -82 -6; peak z-value = 2.09; peak p-value = 0.018; cluster size = 29).

We note that all the correlational effects reported in this section may be affected by low statistical power due to the small sample size. At the same time, we chose to report them, as they illustrate an alternative method to test the correspondence between behavioral and neural effects, which is suggested by analogous patterns in the behavior (the 2BIE; Fig. 1) and the neural response to upright and inverted facing and non-facing dyads (Fig. 3 and 4).

3.1.4. Correlation between the 2BIE and AQ

The above results show that the behavioral 2BIE not only predicts the processing of body dyads in the visual cortex, but also provides a reliable measure of the individual processing of social (multiple-person) scenes, which may be useful to capture interindividual differences. Sensitivity to inversion has been shown to be predictive of the individual's social abilities (Wyer et al., 2012). To study whether a similar relationship can be established for the 2BIE, we performed a correlation between the individual AQ scores and the behavioral 2BIE from session 1. Results revealed a significant negative correlation (Spearman $rho(20) = -0.45$; $p = 0.035$), indicating a smaller 2BIE in individuals with higher scores for autistic traits (*Supplemental Information 4* for correlation analysis using data from session 2).

3.2. Processing of single bodies

3.2.1. The body inversion effect

Configural processing is also thought to apply to single bodies, although the underlying mechanisms appear functionally and anatomically distinct from face-related processing (Yovel and Kanwisher, 2004; Peelen et al., 2006; Peelen and Downing, 2007), and, in many aspects, less clear (Brandman and Yovel, 2012; Brandman and Yovel, 2016). Here, we performed two tests of the body inversion effect as a signature of configural processing. First, in each ROI (table 4), we tested whether the difference in the response to upright bodies *vs.* inverted ones was statistically larger than a general effect of inversion that would be observed for any (non-body) stimulus. In the EBA, we found main effect of category and orientation showing a stronger response to bodies than objects and to upright than inverted stimuli, but no interaction between Category and Orientation. Although the interaction was not significant, pairwise *t*-tests showed greater activity for upright *vs.* inverted bodies [$t(28) = 2.15$, $p = 0.020$], and a trend for a greater response to upright *vs.* inverted objects [$t(28) = 1.56$, $p = 0.065$]. Identical results were found in the FBA [upright *vs.* inverted bodies: $t(28) = 2.30$, $p = 0.015$; upright *vs.* inverted objects: $t(28) = 1.45$, $p = 0.079$] and in the FFA [upright *vs.* inverted bodies: $t(28) = 4.21$, p < 0.001; upright *vs.* inverted objects: $t(28) = 2.30$, p = 0.015]. In the PPA, a main effect of category showed that activity was stronger for objects than for bodies, but there was no effect of orientation or interaction, no difference between upright and inverted bodies [$t(28) = 0.29$, p > 0.250], but a stronger response to upright than inverted objects [$t(28) = 1.71$, $p = 0.049$]. In the EVC, main effects showed a trend for a stronger response to objects than bodies and a stronger response to upright than inverted stimuli, but no interaction, and a stronger response to upright than inverted bodies [$t(28) = 1.99$, $p = 0.028$] and to upright than inverted objects [$t(28) = 2.09$, $p = 0.023$]. In sum, activity was stronger for upright than inverted bodies in all body- and face-specific ROIs considered here (Fig. 5a), but in none of the ROIs the BIE was statistically different from the inversion effect in the neural response to non-body objects.

Further, consistent with the behavioral results, we found that the BIE was smaller than the inversion effect for facing dyads in the EBA, $t(28) = 2.49$, $p = 0.010$, FBA, $t(28) = 1.90$, $p = 0.034$, FFA, $t(28) = 2.01$, $p = 0.027$, and the EVC, $t(28) = 1.71$, $p = 0.049$, but not in PPA, $t(28) = 0.20$, $p > 0.250$. No difference was found between the BIE and the inversion effect for non-facing dyads in any ROI (EBA: $t(28) = 0.96$, $p = 0.174$; FBA: $t(28) = 0.96$, $p = 0.173$; FFA: $t(28) = 0.41$, $p > 0.250$; PPA: $t(28) = 0.56$, $p > 0.250$; EVC: $t(28) = 0.81$, $p = 0.211$).

Using another measure of configural body processing, the discrimination accuracy for upright *vs.* inverted bodies in multivariate pat-

Table 4
Results of the repeated-measures ANOVAs on neural responses (PSC) for the fMRI session with single stimuli.

ROI	Effect	*DF*	*F*	*p*	η_p^2
EBA	Cat.	1,28	160.23	<0.001	0.85
	Orient.	1,28	7.81	0.009	0.22
	Cat. * Orient.	1.28	0.47	*n.s.*	0.02
FBA	Cat.	1,28	38.30	<0.001	0.58
	Orient.	1,28	7.53	0.010	0.21
	Cat. * Orient.	1.28	0.24	*n.s.*	0.01
FFA	Cat.	1,28	41.26	< 0.001	0.60
	Orient.	1,28	23.59	< 0.001	0.46
	Cat. * Orient.	1.28	1.30	*n.s.*	0.04
PPA	Cat.	1,28	46.48	<0.001	0.62
	Orient.	1,28	0.99	*n.s.*	0.03
	Cat. * Orient.	1.28	1.93	0.176	0.06
EVC	Cat.	1,28	4.05	0.054	0.13
	Orient.	1,28	7.56	0.010	0.20
	Cat. * Orient.	1.28	0.19	*n.s.*	0.10

Notes. Cat. = Category; Orient. = Orientation; n.s. = >0.250

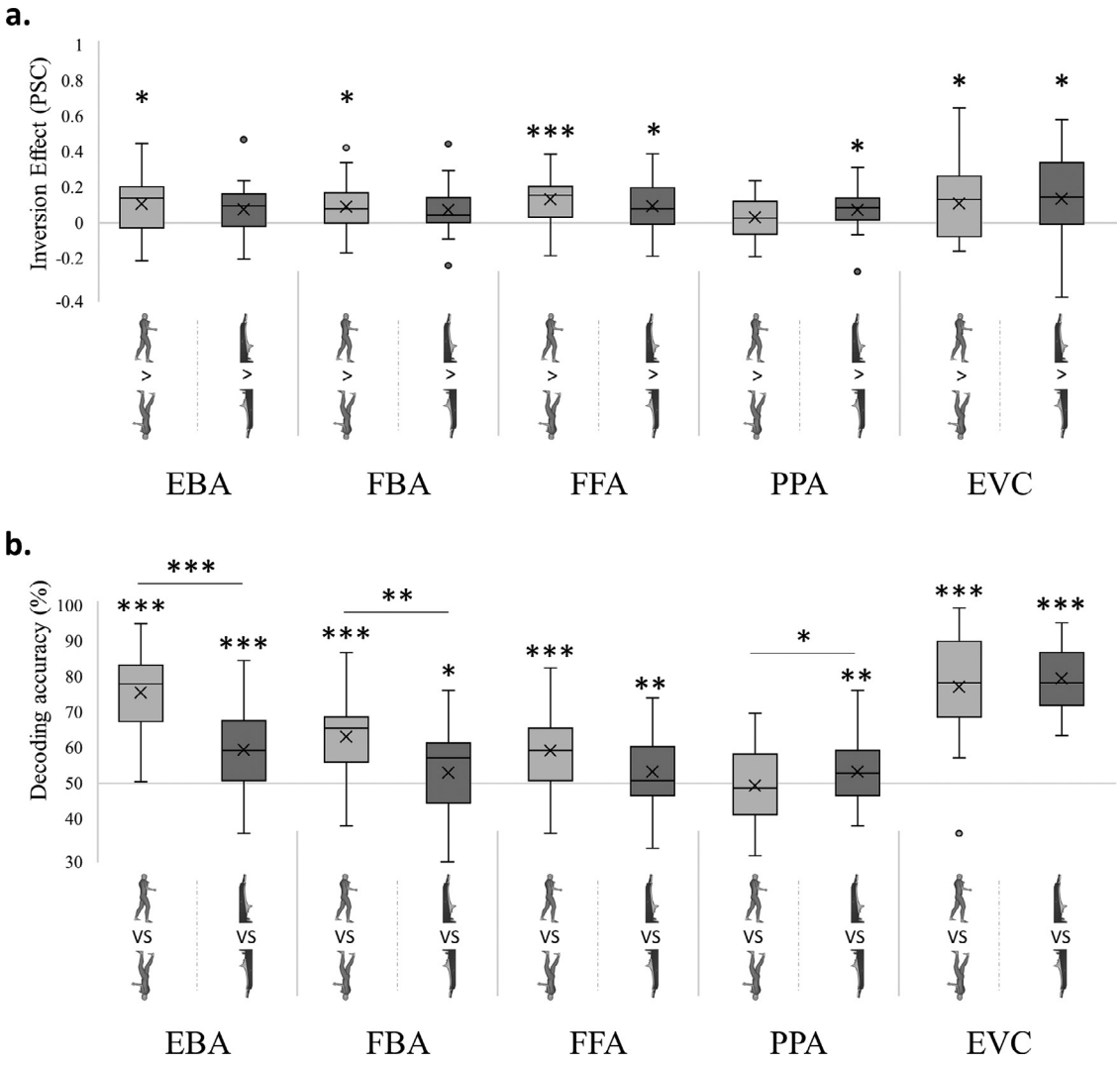

Fig. 5. Neural markers of configural body processing in ROIs. a. Difference in neural activity (PSC) for upright *vs.* inverted stimuli (*i.e.*, inversion effect) for bodies and objects, in each ROI. In no ROI, the inversion effect was larger for bodies than objects. $^{*}p \leq 0.05$; $^{***}p \leq 0.001$; All tests are one-tail *t*-tests. b. Classification accuracies for decoding of upright *vs.* inverted bodies and upright *vs.* inverted objects, in each ROI. Higher decoding accuracy for bodies than objects is taken as a marker of configural processing. Error bars denote the within-subjects normalized SEM. $^{*}p \leq 0.05$; $^{**}p \leq 0.01$; $^{***}p \leq 0.001$; Comparisons against chance level (50 %) and between bodies and objects are performed with one-tail *t*-tests.

Table 5
Mean classification accuracy (± SEM) and significance for the decoding of upright *vs*. inverted single bodies and upright *vs*. inverted single objects as a multivariate test of the inversion effect.

ROI	Bodies			Objects			Comparison between the two	
	Acc.	*t(28)*	*p*	*Acc.*	*t(28)*	*p*	*t(28)*	*p*
EBA	76.80 (± 2.04)	13.16	< 0.001	60.70 (±2.09)	5.12	< 0.001	6.17	< 0.001
FBA	64.22 (± 2.15)	6.61	< 0.001	54.38 (± 1.97)	2.23	0.017	3.20	0.002
FFA	60.42 (± 2.02)	5.15	< 0.001	54.53 (±1.72)	2.63	0.007	2.05	0.025
PPA	50.72 (± 1.95)	0.37	*n.s.*	54.60 (± 1.61)	2.85	0.004	1.90	0.34
EVC	78.02 (± 2.62)	10.70	< 0.001	80.39 (± 1.56)	19.44	< 0.001	0.85	0.202

Notes. Acc = Accuracy; n.s. = >0.250

tern analysis (MVPA) (Brandman and Yovel, 2016), we found more compelling evidence for a BIE in face- and body-specific ROIs. Results showed better decoding accuracy for upright *vs.* inverted stimuli for both body and non-body objects in the EBA, FBA, FFA, EVC, and for non-body objects in the PPA (Fig. 5b; Table 5). We also found that discrimination of multivariate patterns representing upright *vs.* inverted stimuli was more accurate for bodies than for non-body objects in the EBA, FBA and FFA, and more accurate for non-body objects than bodies in the PPA. No difference was found in the EVC. However, correlations between the individual behavioral BIE and the neural BIE yielded no significant effect in any ROI [EBA: $r(20) = -0.10$, $p > 0.250$; FBA: $r(20) = -0.05$, $p > 0.250$; FFA: $r(20) = -0.12$, $p > 0.250$; PPA: $r(20) = 0.88$, $p > 0.250$; EVC: $r(20) = 0.07$, $p > 0.250$], or in any voxel responsive to bodies, across the brain.

4. Discussion

Our findings show that, during processing of multiple bodies, brain areas overlapping with face- and body-specific visual areas encode spatial relations between bodies, yielding different neural responses to face-to-face and back-to-back bodies. In particular, neural responses to facing bodies showed signatures of configural processing, such as stronger activity relative to the response to their scattered version (non-facing dyads), and greater susceptibility to stimulus inversion, which mirrored and correlated with the behavioral 2BIE, taken as a marker of configural processing (Papeo et al., 2017). Finally, we found that the 2BIE was reliable at the individual level, across behavioral sessions and across brain and behavioral measurements, and correlated with the individual's social sensitivity coarsely captured with the AQ.

Configural processing of body dyads. Previous studies have reported increased activity for facing than non-facing dyads in face- and body-specific visual areas (Abassi and Papeo, 2020; Bellot et al., 2021; Walbrin and Koldewyn, 2019). Thus, depending on their relative spatial positioning, the same two bodies are visually processed in different ways. This result is compatible with growing evidence showing that the processing of spatial relations is part of, and affects, the object recognition process (Kaiser et al., 2019; Abassi and Papeo, 2020; Papeo, 2020; Hafri and Firestone, 2021). In addition, here we showed higher sensitivity of the EBA and FFA to the inversion of facing (*vs.* non-facing) dyads. The latter effects suggest that the general increase of neural activity for facing (*vs.* non-facing) dyads may reflect a stronger recruitment of configural processing for facing dyads.

Although there was only a trend for an interaction between Stimulus (facing/non-facing dyads) and Orientation (upright/inverted) in the EBA, this was the only ROI in which the activity was predicted by the performance-based 2BIE measured during the visual-categorization task. This result was confirmed by the whole brain-behavior correlation, which tested every voxel responsive to body-stimuli across the brain, and revealed an effect in the lateral occipital cortex. While correlational results must be taken with caution due to small sample size for this type of analysis, they earned credence as they converged with the results of the univariate whole-brain and ROI analyses, showing analogous patterns in the behavioral response (*i.e.*, the 2BIE) and in the neural response to upright and inverted facing and non-facing dyads, particularly in the EBA and adjacent posterior occipital area (whole-brain and ROI analyses). This effect may reveal uncharted regions of functional specialization for the processing of spatial relations between bodies, or people.

Like the EBA, and in effect, more strongly than the EBA, the FFA showed higher sensitivity to the inversion of facing (relative to non-facing) dyads (*i.e.*, Stimulus by Orientation interaction). Although the activity in this ROI did not correlate with the behavioral 2BIE, the brain-behavior correlation here was not statistically different from the (significant) correlation in the EBA. All other analyses showed that all the effects found in the EBA generalized to the FFA. One possibility is that the FFA response is tied to the processing of faces (and their spatial relations). Faces were clearly visible during fMRI, and less visible, or less attended to, in the visual-categorization task, as in this task subjects were instructed to recognize bodies, which varied in posture but always had the same sketchy head/face (Fig. 1). A version of the visual-categorization task with more emphasis on faces and face processing might yield a stronger brain-behavioral correlation in the FFA.

On this reasoning, the visual processing of spatial relations would be to some extent category-specific, involving the same areas that respond preferentially to the object class implicated in the relation: body-specific areas for bodies, and face-specific areas for faces. However, the recruitment of the FFA in a task that emphasized body processing is also compatible with the view that the FFA is involved in configural analysis of both faces and bodies (Brandman and Yovel, 2016; see also Gauthier et al., 1999; Rhodes et al., 2004). On this view, different response profiles in the FFA and EBA may reflect the implementation of different aspects, or kinds, of configural processing (Yovel et al., 2014; Rezlescu et al., 2017).

The recruitment of configural processing, shown here with the analyses of effects of inversion, opens up further research that should develop new paradigms to test whether other correlates of configural processing found in face and body perception (see Bruyer, 2011; Rezlescu et al., 2017), can also be found in dyad perception. This is especially needed given that research on face perception has characterized the inversion effect as a less direct measure of configural processing than other effects such as the part-whole or the composite effect –while being the best possible predictor of the face recognition performance (Robbins & McKone, 2007; Rezlescu et al., 2017). Providing initial evidence for a part-whole *face-like* effect for facing dyads, Ding et al. (2017) showed that a moving body is recognized better when previously seen interacting in a dyad *versus* in isolation. Likewise, Bellot et al. (2021) showed that two

moving bodies are recognized better when previously seen in a facing dyad than in a non-facing dyad (see also Paparella & Papeo, 2022). Neural counterparts of these effects would be the enhancement of the neural representation of bodies seen in facing dyads, as opposed to the same bodies in a non-facing configuration (Abassi &Papeo, 2020; Bellot et al., 2021), as well as the increase of the neural response to facing (*vs.* non-facing) dyads in visual brain areas, as reported here.

Another open issue concerns the localization of the effects of spatial relations in the brain. It is very likely that the encoding of spatial relations between bodies is not exhausted by the occipitotemporal areas localized in this study. Other relevant area to inspect would be those involved in whole-person perception (Hu et al., 2020), and those involved in motion and action perception (*e.g.*, the posterior superior temporal sulcus), in which sensitivity to spatial relations between bodies has already been reported using dynamic representations of moving bodies (Bellot et al., 2021). In particular, it has been shown that the processing of dynamic facing bodies increased the coupling (*i.e.*, effective connectivity) between body-perception and motion-perception visual areas (*i.e.*, between the EBA and the pSTS) (Bellot et al., 2021). The collective activity of these networks in processing bodies and their relational properties could ultimately be at the service of downstream networks dedicated to the representation of social interaction, and events in general (Isik et al., 2017; Masson et al., 2018; Walbrin et al., 2018; Leshinskaya and Thompson-Schill, 2020; Lee Masson and Isik, 2021).

2BIE and interindividual differences. Face recognition abilities vary across individuals (Dennett et al., 2012; Susilo et al., 2013; Yovel et al., 2014; Wang et al., 2012), but are fairly consistent at the individual level (Rule et al., 2009; Lander et al., 2018; Bate et al., 2019; Ramon et al., 2019), and best predicted by the magnitude of face inversion effect, among the markers of configural face processing (Rezlescu et al., 2017). Evidence for reduced sensitivity to face inversion in ASD subjects has encouraged the thinking that the face inversion effect can be used as a marker of alterations and disease risks that impact social cognition (Farroni and Senju, 2011; Di Giorgio et al., 2016; Neuhaus et al., 2016; Hadad et al., 2019; Van der Donck et al., 2019; Laycock et al., 2020). In this spirit, we showed that, in body-dyad perception, the 2BIE varies across individuals, is reliable over time at the individual level, and correlates with a physiological measure of the same processing (*i.e.*, activity in visual areas for face/body processing; see Elliott et al., 2020). Moreover, we found that the 2BIE correlates with autism-spectrum traits, so that the magnitude of the 2BIE decreases as the AQ score increases. Again, given the limited statistical power of this analysis, evidence for correlation at this point remains anecdotal. Moreover, while we found test-rest reliability and correlations between the two measurements of the 2BIE, we also found evidence for a learning effect that affected the performance in a way that is difficult to characterize. Developing and using different measures of configural processing in dyad perception can help solve this issue in the future. Beyond correlations, the relationship between visual configural processing for body-dyads –as well as for faces and biological motion (Wyer et al., 2012; van Boxtel et al., 2017)– and the set of abilities measured with the AQ, remains unclear. While we work toward confirming and explaining this relationship, behavioral effects that reliably characterize the performance of the individual, highlighting population-level and interindividual differences (see also Pesquita et al., 2022), appear especially worthy of attention as they can offer handy tools for detection of diseases or vulnerabilities. Our results thus encourage further investigation on the clinical significance of the 2BIE as a marker of socially relevant visuoperceptual functions.

Body dyads and single bodies. Targeted as a measure of configural processing, the body inversion effect (BIE) has been demonstrated with behavioral tasks analogous to those used in face perception (Reed et al., 2003, 2006), and effects in the electroencephalography signal (Stekelenburg and De Gelder, 2004; Orlandi and Proverbio, 2020; Adibpour et al., 2021). However, different fMRI measures of the BIE (*e.g.*, neural adaptation or MVPA) have yielded only inconsistent effects of body inversion in the FFA and/or in the EBA (Brandman and Yovel, 2012; Brandman and Yovel, 2016), and some studies have ascribed those effects to the processing of head/face information rather than whole body (Brandman and Yovel, 2010, 2012).

Our results confirm the ambiguity of the BIE and, at the same time, suggest that processing single bodies and processing facing-body dyads could be phenomena of a different nature (different phenomena in kind and/or degree of underlying mechanisms). The BIE showed a cost of inversion that was smaller than the cost for facing dyads (and comparable to the cost for non-facing dyads), both in the behavioral and in the neural responses (in the EBA, FBA and FFA). Moreover, the effect of body inversion in body- and face-specific visual areas was statistically different from a general effect of inversion (*i.e.*, inversion of non-body objects) in the multivariate test (discrimination of upright *vs.* inverted stimuli), but not in the univariate test (level of activity for upright minus inverted bodies) and, in none of the ROIs, it correlated with the behavioral BIE, differently from the 2BIE. Finally, we note that the behavioral 2BIE was correlated with neural activity that partly –but not entirely– overlapped with the EBA, as defined with the classic contrast [single bodies > non-body objects]. This observation encourages the hypothesis that the visual processing of body dyads (especially facing dyads) recruits additional or partly different mechanisms (and neural structures) with respect to the visual processing of single bodies.

5. Conclusions

Using a multimodal approach, we connected behavioral (2BIE) and neural phenomena (greater sensitivity to inversion for facing *vs.* non-facing dyads and larger response to facing *vs.* non-facing dyads), which together suggest the recruitment of configural processing in visual perception of minimal social scenes (facing-body dyads), analogously to what is described for face perception. The recruitment of configural processing implies that facing dyads are processed with the same efficiency and high specialization of other highly familiar or biologically relevant classes of stimuli, such as faces, bodies and biological motion. Our investigation on the 2BIE also shows that this effect could account for the neural responses to body dyad perception, is reliable at the individual level, and correlates with the individual's AQ. The current characterization of the 2BIE thus supports its value as a possible marker of individual visuoperceptual abilities. The visuoperceptual abilities captured by the 2BIE could be precisely those that lay the foundations for living in a social world, for our ability to understand others' relationships and interactions.

Credit author statement

EA and LP contributed equally to this work

Data and Code availability statement

Data and codes for the behavior analyses and fMRI group analyses are available here: https://osf.io/pse3k/

Declaration of Competing Interest

All authors declare that they have no financial or non-financial competing interests.

Data Availability

A link to Data and Codes is provided in the method section

Acknowledgements

This work was supported by a European Research Council Starting Grant to L.P. (Grant number: THEMPO-758473). We thank Nicolas Goupil for contributing to the analyses and editing of Fig. 2.

Supplementary materials

Supplementary material associated with this article can be found, in the online version, at doi:10.1016/j.neuroimage.2022.119506.

References

Abassi, E, Papeo, L, 2020. The representation of two-body shapes in the human visual cortex. J. Neurosci. 40, 852–863. doi:10.1523/JNEUROSCI.1378-19.2019.

Adibpour, P, Hochmann, J-R, Papeo, L, 2021. Spatial relations trigger visual binding of people. J. Cogn. Neurosci. 33, 1343–1353. doi:10.1162/jocn_a_01724.

Ashburner, J, 2007. A fast diffeomorphic image registration algorithm. Neuroimage 38, 95–113. doi:10.1016/j.neuroimage.2007.07.007.

Atkinson, A.P., Heberlein, A.S., Adolphs, R., Adams, R.B., Ambady, N., Nakayama, K., & Shimojo, S. (2011). Are people special? A brain's eye view. Sci. Soc. Vis., 363–392. doi:10.1093/acprof:oso/9780195333176.003.0022.

Axelsson, EL, Buddhadasa, T, Manca, L, Robbins, RA, 2022. Making heads or tails of body inversion effects: do heads matter? PLoS One 17, e0263902. doi:10.1371/journal.pone.0263902.

Baron-Cohen, S., 1997. How to build a baby that can read minds: cognitive mechanisms in mindreading. Maladapt. Mind: Classic Read. Evol. Psychopathol. 207–239.

Baron-Cohen, S, Wheelwright, S, Skinner, R, Martin, J, Clubley, E, 2001. The autism-spectrum quotient (AQ): evidence from Asperger syndrome/high-functioning autism, males and females, scientists and mathematicians. J. Autism Dev. Disord. 31, 5–17. doi:10.1023/A:1005653411471.

Bate, S, Frowd, C, Bennetts, R, Hasshim, N, Portch, E, Murray, E, Dudfield, G, 2019. The consistency of superior face recognition skills in police officers. Appl. Cogn. Psychol. 33, 828–842. doi:10.1002/acp.3525.

Bellot, E, Abassi, E, Papeo, L, 2021. Moving toward *versus* away from another: how body motion direction changes the representation of bodies and actions in the visual cortex. Cereb. Cortex 31, 2670–2685. doi:10.1093/cercor/bhaa382.

Brainard, DH, 1997. The psychophysics toolbox. Spat. Vis. 10, 433–436. doi:10.1163/156856897X00357.

Brambilla, P, Hardan, A, Ucelli Di Nemi, S, Perez, J, Soares, JC, Barale, F, 2003. Brain anatomy and development in autism: Review of structural MRI studies. Brain Res. Bull. 61, 557–569. doi:10.1016/j.brainresbull.2003.06.001.

Brandman, T, Yovel, G, 2010. The body inversion effect is mediated by face-selective, not body-selective. Mechanisms 30, 10534–10540. doi:10.1523/JNEUROSCI.0911-10.2010.

Brandman, T, Yovel, G, 2012. A face inversion effect without a face. Cognition 125, 365–372. doi:10.1016/j.cognition.2012.08.001.

Brandman T, Yovel G (2016) Bodies are represented as wholes rather than their sum of parts in the occipital-temporal cortex. 26(2):530–543. doi:10.1093/cercor/bhu205.

Brett, M, Anton, JL, Valabregue, R, Poline, JB, 2002. Region of interest analysis using a SPM toolbox. 8th International Conference on Functional Mapping of the Human Brain June 2-6, 2002.

Bruyer, R, 2011. Configural face processing: a meta-analytic survey. Perception 40, 1478–1490.

Cook, J, Barbalat, G, Blakemore, SJ, 2012. Top-down modulation of the perception of other people in schizophrenia and autism. Front. Hum. Neurosci. 6, 1–10. doi:10.3389/fnhum.2012.00175.

Dawson, G, Webb, SJ, McPartland, J, 2005. Understanding the nature of face processing impairment in autism: Insights from behavioral and electrophysiological studies. Dev. Neuropsychol. 27, 403–424. doi:10.1207/s15326942dn2703_6.

De Heering, A, & Maurer, D, 2013. The effect of spatial frequency on perceptual learning of inverted faces. Vision research, 86, 107–114. doi:10.1016/j.visres.2013.04.014.

DeGutis, J, Wilmer, J, Mercado, R.J., & Cohan, S, 2013. Using regression to measure holistic face processing reveals a strong link with face recognition ability. Cognition, 126(1), 87–100. doi:10.1016/j.cognition.2012.09.004.

Dennett, HW, McKone, E, Edwards, M, Susilo, T, 2012. Face aftereffects predict individual differences in face recognition ability. Psychol. Sci. 23, 1279–1287. doi:10.1177/0956797612446350.

Desikan, RS, Ségonne, F, Fischl, B, Quinn, BT, Dickerson, BC, Blacker, D, Buckner, RL, Dale, AM, Maguire, RP, Hyman, BT, Albert, MS, Killiany, RJ, 2006. An automated labeling system for subdividing the human cerebral cortex on MRI scans into gyral based regions of interest. Neuroimage 31, 968–980. doi:10.1016/j.neuroimage.2006.01.021.

Ding, X, Gao, Z, Shen, M, 2017. Two equals one: two human actions during social interaction are grouped as one unit in working memory. Psychol. Sci. 28, 1311–1320. doi:10.1177/0956797617707318.

Di Giorgio, E, Frasnelli, E, Rosa Salva, O, Maria Luisa, S, Puopolo, M, Tosoni, D, Simion, F, Vallortigara, G, Apicella, F, Gagliano, A, Guzzetta, A, Molteni, M, Persico, A, Pioggia, G, Valeri, G, Vicari, S, 2016. Difference in visual social predispositions between newborns at Low-and High-risk for Autism. Sci. Rep. 6, 1–9. doi:10.1038/srep26395.

Duchaine, B, Nakayama, K, 2006. The cambridge face memory test: results for neurologically intact individuals and an investigation of its validity using inverted face stimuli and prosopagnosic participants. Neuropsychologia 44, 576–585. doi:10.1016/j.neuropsychologia.2005.07.001.

Eickhoff, SB, Stephan, KE, Mohlberg, H, Grefkes, C, Fink, GR, Amunts, K, Zilles, K, 2005. A new SPM toolbox for combining probabilistic cytoarchitectonic maps and functional imaging data. Neuroimage 25, 1325–1335. doi:10.1016/j.neuroimage.2004.12.034.

Elliott, ML, Knodt, AR, Ireland, D, Morris, ML, Poulton, R, Ramrakha, S, Sison, ML, Moffitt, TE, Caspi, A, Hariri, AR, 2020. What is the test-retest reliability of common task-functional MRI measures? New empirical evidence and a meta-analysis. Psychol. Sci. 31, 792–806. doi:10.1177/0956797620916786.

Farroni, T., Senju, A., 2011. Specialized brain for the social vision: perspectives from typical and atypical development. Social Vision 421–443. doi:10.1093/acprof:oso/9780195333176.003.0025.

Fischl, B, 2012. FreeSurfer. Neuroimage 62, 774–781. doi:10.1016/j.neuroimage.2012.01.021.

Friston, KJ, Williams, S, Howard, R, Frackowiak, RSJ, Turner, R, 1996. Movement-related effects in fMRI time-series. Magn. Reson. Med. 35, 346–355. doi:10.1002/mrm.1910350312.

Friston, KJ, Ashburner, J, Kiebel, S, Nichols, T, Penny, WD, 2007. Statistical Parametric Mapping : The Analysis of Funtional Brain Images. Elsevier/Academic Press.

Gauthier, I, Tarr, MJ, Anderson, AW, Skudlarski, P, Gore, JC, 1999. Activation of the middle fusiform ' face area ' increases with expertise in recognizing novel objects. Nat. Neurosci. 2 (6), 568–573. doi:10.1038/9224.

Hadad, BS, Schwartz, S, Binur, N, 2019. Reduced perceptual specialization in autism: Evidence from the other-race face effect. J. Exp. Psychol. Gen. 148, 588–594. doi:10.1037/xge0000550.

Hu, Y, Baragchizadeh, A, & O'Toole, A.J., 2020. Integrating faces and bodies: Psychological and neural perspectives on whole person perception. Neuroscience & Biobehavioral Reviews, 112, 472–486. doi:10.1016/j.neubiorev.2020.02.021.

Hafri, A, Firestone, C, 2021. The perception of relations. Trends Cogn. Sci. 1–18. doi:10.1016/j.tics.2021.01.006.

Hussain, Z, Sekuler, A.B., & Bennett, P.J., 2009. Perceptual learning modifies inversion effects for faces and textures. Vision research, 49(18), 2273-2284. doi:10.1016/j.visres.2009.06.014.

Isik, L, Koldewyn, K, Beeler, D, Kanwisher, N, 2017. Perceiving social interactions in the posterior superior temporal sulcus. Proc Natl Acad Sci doi:10.1073/pnas.1714471114.

Jenkinson, M, Beckmann, CF, Behrens, TEJ, Woolrich, MW, Smith, SM, 2012. FSL. Neuroimage 62, 782–790. doi:10.1016/j.neuroimage.2011.09.015.

Johnson, CP, 2004. New tool helps primary care physicians diagnose autism early. AAP News 24 (2), 74. https://www.aappublications.org/content/24/2/74.

Kaiser, D, Quek, GL, Cichy, RM, Peelen, M.V., 2019. Object vision in a structured world. Trends Cogn. Sci. 23, 672–685. doi:10.1016/j.tics.2019.04.013.

Lander, K, Bruce, V, Bindemann, M, 2018. Use-inspired basic research on individual differences in face identification: implications for criminal investigation and security. Cogn. Res. Princ. Implic. 3, 1–13. doi:10.1186/s41235-018-0115-6.

Laguesse, R, Dormal, G, Biervoye, A, Kuefner, D, & Rossion, B, 2012. Extensive visual training in adulthood significantly reduces the face inversion effect. Journal of vision, 12(10), 14–14. doi:10.1167/12.10.14.

Laycock, R, Wood, K, Wright, A, Crewther, SG, Goodale, MA, 2020. Saccade latency provides evidence for reduced face inversion effects with higher autism traits. Front. Hum. Neurosci. 13. doi:10.3389/fnhum.2019.00470.

Lee IA, Preacher KJ (2013) Calculation for the test of the difference between two dependent correlations with one variable in common. http://quantpsy.org/corrtest/corrtest2.htm

Lee Masson, H, Isik, L, 2021. Functional selectivity for social interaction perception in the human superior temporal sulcus during natural viewing. Neuroimage 245, 118741. doi:10.1016/j.neuroimage.2021.118741.

Leshinskaya, A, Thompson-Schill, SL, 2020. Transformation of event representations along middle temporal Gyrus. Cereb Cortex (New York, NY) 30, 3148. doi:10.1093/cercor/bhz300.

Masson HL, Plas S Van De, Daniels N, Beeck H Op De (2018) NeuroImage the multidimensional representational space of observed socio-affective touch experiences. 175:297–314. https://doi.org/10.1016/j.neuroimage.2018.04.007

Maurer, D, Le Grand, R, Mondloch, CJ, 2002. The many faces of configural processing. Trends Cogn. Sci. 6, 255–260. doi:10.1016/s1364-6613(02)01903-4.

Neuhaus, E, Jones, EJH, Barnes, K, Sterling, L, Estes, A, Munson, J, Dawson, G, Webb, SJ, 2016. The relationship between early neural responses to emotional faces at age 3 and later autism and anxiety symptoms in adolescents with Autism. J. Autism Dev. Disord. 46, 2450–2463. doi:10.1007/s10803-016-2780-y.

Nichols, TE, Holmes, AP, 2002. Nonparametric permutation tests for functional neuroimaging: a primer with examples. Hum. Brain Mapp. 15 (1), 1–25. doi:10.1002/hbm.1058.

Oosterhof, NN, Connolly, AC, Haxby, J.V., 2016. CoSMoMVPA: multi-modal multivariate pattern analysis of neuroimaging data in Matlab/GNU Octave. Front. Neuroinform. 10, 1–27. doi:10.3389/fninf.2016.00027.

Orlandi, A, Proverbio, AM, 2020. ERP indices of an orientation-dependent recognition of the human body schema. Neuropsychologia 146, 107535. doi:10.1016/j.neuropsychologia.2020.107535.

Paparella, I, Papeo, L, 2022. Chunking by social relationship in working memory. Visual Cognit. 30, 354–370. doi:10.1080/13506285.2022.2064950.

Papeo, L, 2020. Twos in human visual perception. Cortex 132, 473–478. doi:10.1016/j.cortex.2020.06.005.

Papeo, L, Abassi, E, 2019. Seeing social events: the visual specialization for dyadic human–human interactions. J. Exp. Psychol. Hum. Percept. Perform. 45, 877–888. doi:10.1037/xhp0000646.

Papeo, L, Stein, T, Soto-Faraco, S, 2017. The two-body inversion effect. Psychol. Sci. 28, 369–379. doi:10.1177/0956797616685769.

Peelen, M.V., Wiggett, AJ, Downing, PE, 2006. Patterns of fMRI activity dissociate overlapping functional brain areas that respond to biological motion. Neuron 49, 815–822. doi:10.1016/j.neuron.2006.02.004.

McCarthy, P, 2022. FSLeyes (1.4.0). Zenodo. doi:10.5281/zenodo.6511596.

Peelen M V, Downing PE (2007) The neural basis of visual body perception. 8:636–648. doi:10.1038/nrn2195.

Pesquita, A, Rennels, JL, Bernardet, U, Richards, BE, Jensen, O, Shapiro, K, 2022. Isolating action prediction from action integration in the perception of social interactions. Brain Sci. 12, 432. doi:10.3390/brainsci12040432, 2022Page12:432.
Powell, LJ, Spelke, ES, 2018. Human infants' understanding of social imitation: inferences of affiliation from third party observations. Cognition 170, 31–48. doi:10.1016/j.cognition.2017.09.007.
Quadflieg, S, Koldewyn, K, 2017. The neuroscience of people watching: How the human brain makes sense of other people's encounters. Ann N Y Acad Sci 1396, 166–182. doi:10.1111/nyas.13331.
Ramon, M, Bobak, AK, White, D, 2019. Super-recognizers: from the lab to the world and back again. Br. J. Psychol. 110, 461–479. doi:10.1111/bjop.12368.
Reed, CL, Stone, VE, Bozova, S, Tanaka, J, 2003. The body-inversion effect. Psychol. Sci. 14, 302–308. doi:10.1111/1467-9280.14431.
Reed, CL, Stone, VE, Grubb, JD, McGoldrick, JE, 2006. Turning configural processing upside down: part and whole body postures. J. Exp. Psychol. Hum. Percept. Perform. 32, 73–87. doi:10.1037/0096-1523.32.1.73.
Rezlescu, C, Chapman, A, Susilo, T, Caramazza, A, 2016. Large inversion effects are not specific to faces and do not vary with object expertise. PsyArXiv doi:10.31234/osf.io/xzbe5.
Rezlescu, C, Wilmer, JB, Caramazza, A, 2017. The inversion, part-whole, and composite effects reflect distinct perceptual mechanisms with varied relationships to face recognition. J. Exp. Psychol. Hum. Percept. Perform. 43 (12), 1961. doi:10.1037/xhp0000400.
Rhodes, G, Byatt, G, Michie, PT, Puce, A, 2004. Is the fusiform face area specialized for faces, individuation, or expert individuation? J. Cogn. Neurosci. 16, 189–203. doi:10.1162/089892904322984508.
Robbins, R, Mckone, E, 2007. No face-like processing for objects-of-expertise in three behavioural tasks. Cognition 103, 34–79. doi:10.1016/j.cognition.2006.02.008.
Rossion, B, Delvenne, JF, Debatisse, D, Goffaux, V, Bruyer, R, Crommelinck, M, Guérit, JM, 1999. Spatio-temporal localization of the face inversion effect: an event-related potentials study. Biol. Psychol. 50, 173–189. doi:10.1016/S0301-0511(99)00013-7.
Rossion, B, Gauthier, I, Tarr, MJ, Despland, P, Bruyer, R, Linotte, S, Crommelinck, M, 2000. The N170 occipito-temporal component is delayed and enhanced to inverted faces but not to inverted objects: an electrophysiological account of face-specific processes in the human brain. Neuroreport 11, 69–74. doi:10.1097/00001756-200001170-00014.
Rule, NO, Ambady, N, Adams, RB, 2009. Personality in perspective: judgmental consistency across orientations of the face. Perception 38, 1688–1699. doi:10.1068/p6384.
Ruzich, Emily, Allison, Carrie, Smith, P, Watson, P, et al., 2015. Measuring autistic traits in the general population: a systematic review of the Autism-Spectrum Quotient (AQ) in a nonclinical population sample of 6,900 typical adult males and females. Mol. Autism 6, 1–12. doi:10.1186/2040-2392-6-2.
Sadeh, B, Yovel, G, 2010. Why is the N170 enhanced for inverted faces? An ERP competition experiment. Neuroimage 53, 782–789. doi:10.1016/j.neuroimage.2010.06.029.
Simmons, DR, Robertson, AE, McKay, LS, Toal, E, McAleer, P, Pollick, FE, 2009. Vision in autism spectrum disorders. Vis. Res. 49, 2705–2739. doi:10.1016/j.visres.2009.08.005.
Smith, SM, Nichols, TE, 2009. Threshold-free cluster enhancement: addressing problems of smoothing, threshold dependence and localisation in cluster inference. Neuroimage 44, 83–98. doi:10.1016/j.neuroimage.2008.03.061.
Soares, JM, Magalhães, R, Moreira, PS, Sousa, A, Ganz, E, Sampaio, A, Alves, V, Marques, P, Sousa, N, 2016. A Hitchhiker's guide to functional magnetic resonance imaging. Front. Neurosci. 10, 515. doi:10.3389/fnins.2016.00515.
Steiger, JH, 1980. Tests for comparing elements of a correlation matrix. Psychol. Bull. 87, 245–251. doi:10.1037/0033-2909.87.2.245, Available at: /record/1980-08757-001.
Stekelenburg, JJ, De Gelder, B, 2004. The neural correlates of perceiving human bodies: an ERP study on the body-inversion effect. Neuroreport 15, 777–780. doi:10.1097/00001756-200404090-00007.
Stigliani, A, Weiner, KS, Grill-Spector, K, 2015. Temporal processing capacity in high-level visual cortex is domain specific. J. Neurosci. 35, 12412–12424. doi:10.1523/jneurosci.4822-14.2015.
Susilo, T, Germine, L, Duchaine, B, 2013. Face recognition ability matures late: Evidence from individual differences in young adults. J. Exp. Psychol. Hum. Percept. Perform. 39, 1212–1217. doi:10.1037/a0033469.
Tanaka, JW, Farah, MJ, 1993. Parts and wholes in face recognition. Q. J. Exp. Psychol. Sect. A 46, 225–245. doi:10.1080/14640749308401045.
Taylor, JC, Wiggett, AJ, Downing, PE, 2007. Functional MRI analysis of body and body part representations in the extrastriate and fusiform body areas. J. Neurophysiol. 98, 1626–1633. doi:10.1152/jn.00012.2007.
Thornton (2016). Introducing MatlabTFCE. http://markallenthornton.com/blog/matlab-tfce/https://github.com/markallenthornton/MatlabTFCE
Troje, NF, Westhoff, C, 2006. The inversion effect in biological motion perception: evidence for a "Life Detector"? Curr. Biol. 16, 821–824. doi:10.1016/j.cub.2006.03.022.
van Boxtel, JJA, Peng, Y, Su, J, Lu, H, 2017. Individual differences in high-level biological motion tasks correlate with autistic traits. Vision Res. 141, 136–144. doi:10.1016/j.visres.2016.11.005.
Van der Donck, S, Dzhelyova, M, Vettori, S, Thielen, H, Steyaert, J, Rossion, B, Boets, B, 2019. Fast periodic visual stimulation EEG reveals reduced neural sensitivity to fearful faces in children with Autism. J. Autism Dev. Disord. 49, 4658–4673. doi:10.1007/s10803-019-04172-0.
Walbrin, J, Downing, P, Koldewyn, K, 2018. Neural responses to visually observed social interactions. Neuropsychologia 112, 31–39. doi:10.1016/j.neuropsychologia.2018.02.023.
Walbrin, J, Koldewyn, K, 2019. Dyadic interaction processing in the posterior temporal cortex. Neuroimage 198, 296–302. doi:10.1016/j.neuroimage.2019.05.027.
Wang, R, Li, J, Fang, H, Tian, M, Liu, J, 2012. Individual differences in holistic processing predict face recognition ability. Psychol. Sci. 23, 169–177. doi:10.1177/0956797611420575.
Webb, SJ, Neuhaus, E, Faja, S, 2017. Face perception and learning in autism spectrum disorders. Q. J. Exp. Psychol. 70, 970–986. doi:10.1080/17470218.2016.1151059.
Vettori, S, Dzhelyova, M, Van der Donck, S, Jacques, C, Steyaert, J, Rossion, B, Boets, B, 2019b. Reduced neural sensitivity to rapid individual face discrimination in autism spectrum disorder. NeuroImage Clin. 21, 101613. doi:10.1016/j.nicl.2018.101613.
Wyer, NA, Martin, D, Pickup, T, Neil Macrae, C, 2012. Individual differences in (Non-Visual) processing style predict the face inversion effect. Cogn. Sci. 36, 373–384. doi:10.1111/j.1551-6709.2011.01224.x.
Yin, RK, 1969. Looking at upside-down faces. J. Exp. Psychol. 81, 141–145. https://psycnet.apa.org/doi/10.1037/h0027474.
Yovel, G, Kanwisher, N, 2004. Face perception : domain specific, not process specific. Neuron 44 (5), 889–898. doi:10.1016/j.neuron.2004.11.018.
Yovel, G, Kanwisher, N, 2005. The neural basis of the behavioral face-inversion effect. Curr. Biol. 15, 2256–2262. doi:10.1016/j.cub.2005.10.072.
Yovel, G, Wilmer, JB, Duchaine, B, 2014. What can individual differences reveal about face processing? Front. Hum. Neurosci. 8, 1–9. doi:10.3389/fnhum.2014.00562.